USGS
science for a changing world

Numerical Modeling of the Effects of Hurricane Sandy and Potential Future Hurricanes on Spatial Patterns of Salt Marsh Morphology in Jamaica Bay, New York City

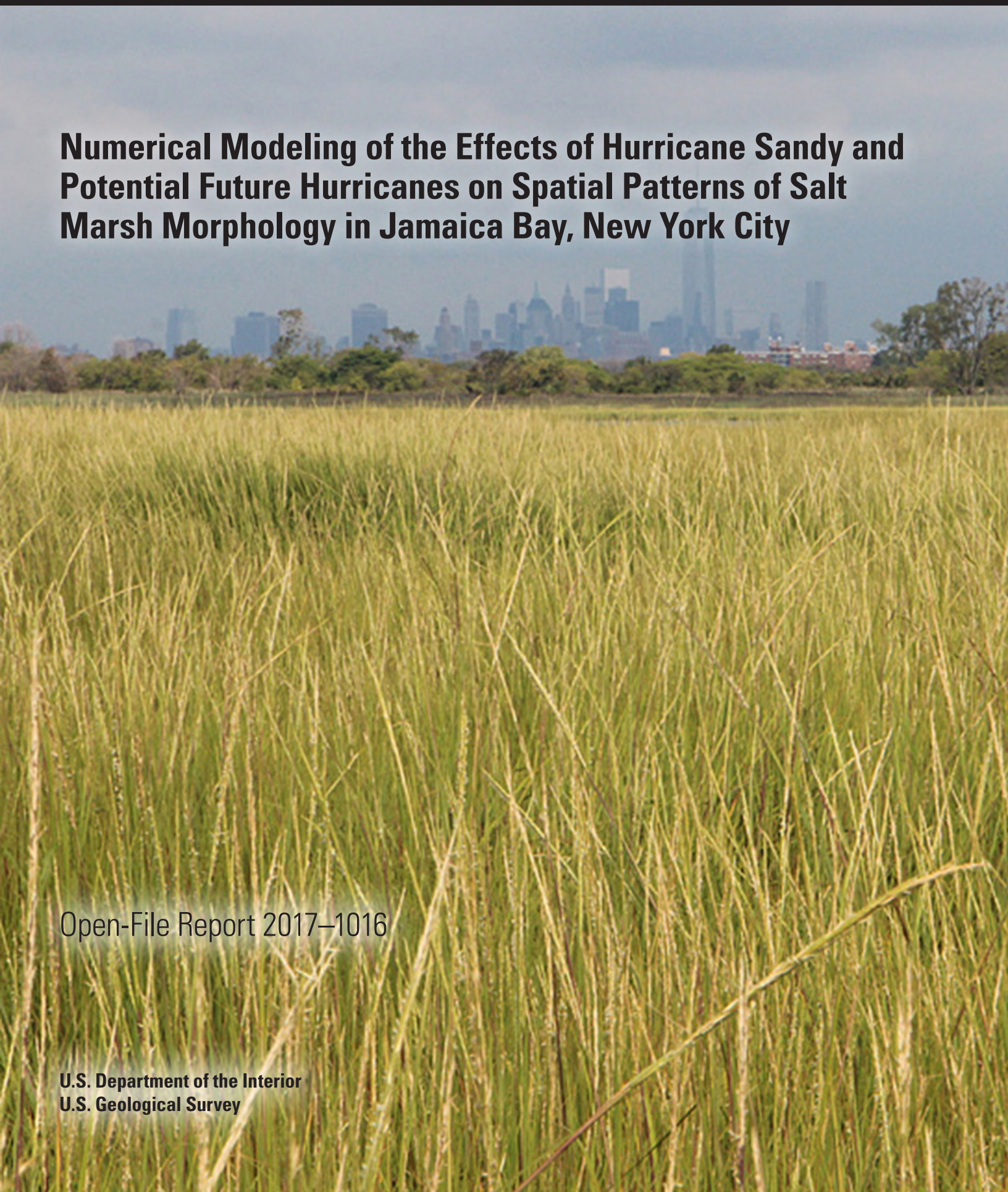

Open-File Report 2017–1016

U.S. Department of the Interior
U.S. Geological Survey

Cover. Manhattan skyline as seen from Yellow Bar, Jamaica Bay, New York. Photograph by Don Riepe, American Littoral Society, used with permission.

Numerical Modeling of the Effects of Hurricane Sandy and Potential Future Hurricanes on Spatial Patterns of Salt Marsh Morphology in Jamaica Bay, New York City

By Hongqing Wang, Qin Chen, Kelin Hu, Gregg A. Snedden, Ellen K. Hartig, Brady R. Couvillion, Cody L. Johnson, and Philip M. Orton

Open-File Report 2017–1016

U.S. Department of the Interior
U.S. Geological Survey

U.S. Geological Survey
William H. Werkheiser, Acting Director

U.S. Geological Survey, Reston, Virginia: 2017

For more information on the USGS—the Federal source for science about the Earth, its natural and living resources, natural hazards, and the environment—visit http://www.usgs.gov or call 1–888–ASK–USGS.

For an overview of USGS information products, including maps, imagery, and publications, visit http://store.usgs.gov.

Suggested citation:
Wang, H., Chen, Q., Hu, K., Snedden, G.A., Hartig, E.K., Couvillion, B.R., Johnson, C.L., and Orton, P.M., 2017, Numerical modeling of the effects of Hurricane Sandy and potential future hurricanes on spatial patterns of salt marsh morphology in Jamaica Bay, New York City: U.S. Geological Survey Open-File Report 2017–1016, 43 p., https://doi.org/10.3133/ofr20171016.

ISSN 2331-1258 (online)

Acknowledgments

We thank Leah Bechett, Theresa Crupi, Chris Haight, Charuta Kulkarni, and Rebecca Swadek of the New York City Department of Parks & Recreation, Jessica Browning, George Frame, and Patricia Rafferty of the National Park Service, and Ian MacColl, Don Riepe, Elizabeth Stoehr of the American Littoral Society for assistance in field sampling and measurements. Mark Christiano of the National Park Service, William Jones of the U.S. Geological Survey, and Yeqiao Wang of the University of Rhode Island provided Jamaica Bay vegetation distribution data. Sam Bentley, Thomas Blanchard, Ryan Clarke, Haoran Liu, Crawford White, and Kevin Xu of Louisiana State University provided laboratory analysis. James Lynch of the National Park Service provided SET and marker horizon data and technical support. Qinghua Ye from Deltares provided technical assistance for using the Delft3D model. Jeffrey Danielson and Dean Tyler of the U.S. Geological Survey provided the Coastal National Elevation Database (CoNED) with updated topography and bathymetry data for the Jamaica Bay area.

We are grateful to Alex Kolker of the Louisiana Universities Marine Consortium, Marit Larson of the New York City Department of Parks & Recreation, Alisha Renfro of the National Wildlife Federation, and Matthew Andersen, Donald Cahoon, Thomas Doyle, and Gregory Steyer of the U.S. Geological Survey for discussions about the ecological issues in Jamaica Bay, strategies in modeling sediment transport in coastal wetlands, and the role of vegetation in sediment transport and morphology. We would like to thank Julie Rosati of the U.S. Army Corps of Engineers and Eric Swain of the U.S. Geological Survey for their constructive reviews of this report.

Contents

Figures

Tables

Conversion Factors

International System of Units to U.S. customary units

Multiply	By	To obtain
	Length	
micrometer (µm)	0.0000394	inch (in.)
millimeter (mm)	0.03937	inch (in.)
centimeter (cm)	0.3937	inch (in.)
meter (m)	3.281	foot (ft)
meter (m)	1.094	yard (yd)
kilometer (km)	0.6214	mile (mi)
kilometer (km)	0.5400	mile, nautical (nmi)
	Area	
square meter (m^2)	0.0002471054	acre
square kilometer (km^2)	247.1	acre
square kilometer (km^2)	0.3861	square mile (mi^2)
	Volume	
cubic meters (m^3)	35.31	cubic foot (ft^3)
cubic kilometers (km^3)	0.239913	cubic mile (mi^3)
	Velocity	
meter per second (m/s)	3.281	foot per second (ft/s)
	Kinematic viscosity	
square meter per second (m^2/s)	10.7639	square foot per second (ft^2/s)
	Density	
kilogram per cubic meter (kg/m^3)	0.062428	pound per cubic foot (lb/ft^3)
	Mass	
metric ton (t)	2,204.62	pound (lb)
	Pressure	
kilopascal (kPa)	0.00986923	atmosphere, standard (atm)
kilopascal (kPa)	20.885472	pound per square foot (lb/ft^2)

Datums

Horizontal coordinate information is referenced to the North American Datum of 1983 (NAD 83).
Vertical coordinate information is referenced to the North American Vertical Datum of 1988 (NAVD 88).

Numerical Modeling of the Effects of Hurricane Sandy and Potential Future Hurricanes on Spatial Patterns of Salt Marsh Morphology in Jamaica Bay, New York City

By Hongqing Wang,[1] Qin Chen,[2] Kelin Hu,[2] Gregg A. Snedden,[1] Ellen K. Hartig,[3] Brady R. Couvillion,[1] Cody L. Johnson,[2] and Philip M. Orton[4]

Abstract

The salt marshes of Jamaica Bay, managed by the New York City Department of Parks & Recreation and the Gateway National Recreation Area of the National Park Service, serve as a recreational outlet for New York City residents, mitigate flooding, and provide habitat for critical wildlife species. Hurricanes and extra-tropical storms have been recognized as one of the critical drivers of coastal wetland morphology due to their effects on hydrodynamics and sediment transport, deposition, and erosion processes. However, the magnitude and mechanisms of hurricane effects on sediment dynamics and associated coastal wetland morphology in the northeastern United States are poorly understood. In this study, the depth-averaged version of the Delft3D modeling suite, integrated with field measurements, was utilized to examine the effects of Hurricane Sandy and future potential hurricanes on salt marsh morphology in Jamaica Bay, New York City. Hurricane Sandy-induced wind, waves, storm surge, water circulation, sediment transport, deposition, and erosion were simulated by using the modeling system in which vegetation effects on flow resistance, surge reduction, wave attenuation, and sedimentation were also incorporated. Observed marsh elevation change and accretion from a rod surface elevation table and feldspar marker horizons and cesium-137- and lead-210-derived long-term accretion rates were used to calibrate and validate the wind-waves-surge-sediment transport-morphology coupled model.

The model results (storm surge, waves, and marsh deposition and erosion) agreed well with field measurements. The validated modeling system was then used to detect salt marsh morphological change due to Hurricane Sandy across the entire Jamaica Bay over the short-term (for example, 4 days and 1 year) and long-term (for example, 5 and 10 years). Because Hurricanes Sandy (2012) and Irene (2011) were two large and destructive tropical cyclones which hit the northeast coast, the validated coupled model was run to predict the effects of Sandy-like and Irene-like hurricanes with different storm tracks and wind intensities on wetland morphology in Jamaica Bay. Model results indicate that, in Jamaica Bay salt marshes, the morphological changes (greater than 5 millimeters [mm] determined by the long-term marsh accretion rate) caused by Hurricane Sandy were complex and spatially heterogeneous. Most of the erosion (5–40 mm) and deposition (5–30 mm) were mainly characterized by fine sand for channels and bay bottoms and by mud for marsh areas. Hurricane Sandy-generated deposition and erosion were generated locally. The storm-induced net sediment input through Rockaway Inlet was only about 1 percent of the total amount of the sediment reworked by the hurricane. Salt marshes inside the western part of the bay showed erosion overall while marshes inside the eastern part showed deposition from Hurricane Sandy. Model results indicated that most of the marshes could recover from Hurricane Sandy-induced erosion after 1 year and demonstrated continued marsh accretion after the hurricane over the course of long simulation periods although the effect (accretion) was diminished. Local waves and currents generated by Hurricane Sandy appeared to play a critical role in sediment transport and associated wetland morphological change in Jamaica Bay. Hypothetical hurricanes, depending on their track and intensity, cause variable responses in spatial patterns of sediment deposition and erosion compared to simulations without the hurricane. In general, hurricanes passing west of the Jamaica Bay estuary appear to be more destructive to the salt marshes than those passing the east. Consequently, marshes inside the western part of the bay were likely to be more vulnerable to hurricanes than marshes inside the eastern part of the bay.

[1]U.S. Geological Survey.

[2]Louisiana State University, Baton Rouge, LA, USA.

[3]New York City Department of Parks & Recreation, NY, USA.

[4]Stevens Institute of Technology, Hoboken, NJ, USA.

Introduction

With Congressional funding provided to the Department of the Interior following Hurricane Sandy in 2012, the U.S. Geological Survey (USGS) conducted an interdisciplinary study to develop a wetland-hurricane modeling system to assess and predict the short- and long-term effects of Hurricane Sandy and hypothetical hurricanes on wetland morphology in Jamaica Bay, New York City, New York. This study was one of the projects of Theme 5: Impacts to Coastal Ecosystems, Habitats, and Fish and Wildlife of the USGS's response to Hurricane Sandy. This research was a large collaborative effort among USGS, Louisiana State University, New York City Department of Parks & Recreation, National Park Service, and Stevens Institute of Technology.

Jamaica Bay Estuary

The Jamaica Bay estuary is located in Brooklyn and Queens, New York City, on the western end of the south shore of the Long Island land mass (fig. 1). It covers about 107 square kilometers (km^2) and opens into the Atlantic Ocean by way of Rockaway Inlet on the southwest. Jamaica Bay Wildlife Refuge (JBWR), part of the National Park Service-Gateway National Recreation Area (NPS-GNRA), is located within Jamaica Bay. Established in 1972, GNRA is the Nation's first urban national park and the largest tidal wetland complex in the New York metropolitan area. Some fringing marshes are located outside the wildlife refuge and lie outside the GNRA boundaries. These are managed by the New York City Department of Parks & Recreation (Hartig and others, 2002). Jamaica Bay consists of narrow channels and tidal marsh islands that are exposed during low tides (tide range is about 1.6 meters [m]). Navigable channels, approximately 10 m in depth, encircle most of the outer ring of the bay. Navigable tributaries, such as Pumpkin Patch Channel and Broad Channel, connect to the main channels, which include North Channel, Island Channel, and Beach Channel (fig. 2). Tidal exchange with the Atlantic Ocean is through Rockaway Inlet (figs. 1 and 2).

Jamaica Bay is an estuary with diverse habitats, including open water, coastal shoals, bars, mudflats, intertidal salt marshes, and upland areas. It provides critical ecological and economic value to the State of New York and the nation. Prior to 1865, Jamaica Bay was known for its abundance and diversity of shellfish as well as its importance as a nursery and feeding ground for many species of birds and fish because of its extensive marsh islands, tidal creeks, mudflats, and brackish water (Brown, 1981). However, extensive anthropogenic activities have altered Jamaica Bay. For example, natural flow of water and sediment into the bay has been affected by residential, commercial, and transportation development, channel dredging, stormwater runoff diversion, and sewage treatment plant operations (Kolker, 2005; Benotti and others, 2007; Swanson and Wilson, 2008; Talke and others, 2014; Wigand and others, 2014).

From 1924 to 1999, Jamaica Bay experienced a conversion of more than 50 percent of its vegetated saltmarsh islands into nonvegetated intertidal and subtidal mudflats (Hartig and others, 2002). Between 1951 and 2008, about 6.5 km^2 of salt marsh were lost, about 0.125 square kilometers per year (km^2/yr; Rafferty and others, 2011); the present rate of loss has increased to 0.16–0.20 km^2/yr (Harmon, 2006). Marsh losses prior to the GNRA's establishment were mainly the result of direct dredging and filling activity in wetlands; the more recent losses are from marsh erosion (fig. 3) and inundation. It has been predicted that without further restoration, management, and protection actions, salt marshes in Jamaica Bay will disappear by 2024 (Steinberg and others, 2004).

The stressors contributing to marsh loss in Jamaica Bay include (1) increases in the frequency and duration of marsh flooding and tidal hydrodynamics due to anthropogenic changes to the tidal range (Swanson and Wilson, 2008; Talke and others, 2014); (2) sea-level rise (2.77 millimeters per year [mm/yr] at the Battery tide gage station during 1856–1996, Hartig and others, 2002; and recently 3.05 mm/yr during 1900–2013, Horton and others, 2015); (3) shallow subsidence in part due to reduced root production caused by nutrient, particularly nitrogen, overloading (Benotti and others, 2007; Wigand and others, 2014); (4) insufficient sediment supply from marine and riverine sources and significant amounts of sediment trapped in deep "borrow pits" rather than being transported to the marsh surface (starving salt marshes), among others (Rafferty and others, 2011). Some research has shown that although climate is an important driver of mineral deposition and accretion, accretion rates do not appear to be related to salt marsh loss in the bay and seem to be related to eutrophication and organic matter inputs (for example, Kolker, 2005). Nevertheless, the magnitude and mechanism of marsh erosion both vertically and laterally under climate change and human disturbance are rarely studied simultaneously with marsh accretion. Additionally, variations in bathymetry, tidal range, circulation patterns, and climate (for example, wind speed, wind direction, the fetch, wave height, and wave direction) and vegetation distribution may affect sediment (re)suspension, transport, settling, deposition, erosion, retention and marsh accretion and erosion. All of these are expected to show spatial variability (Kolker, 2005; Liu and others, 2015), resulting in accretion rates sufficient to keep pace with the relative sea-level rise (RSLR) at some marsh sites but insufficient to keep pace with the RSLR in other marsh sites.

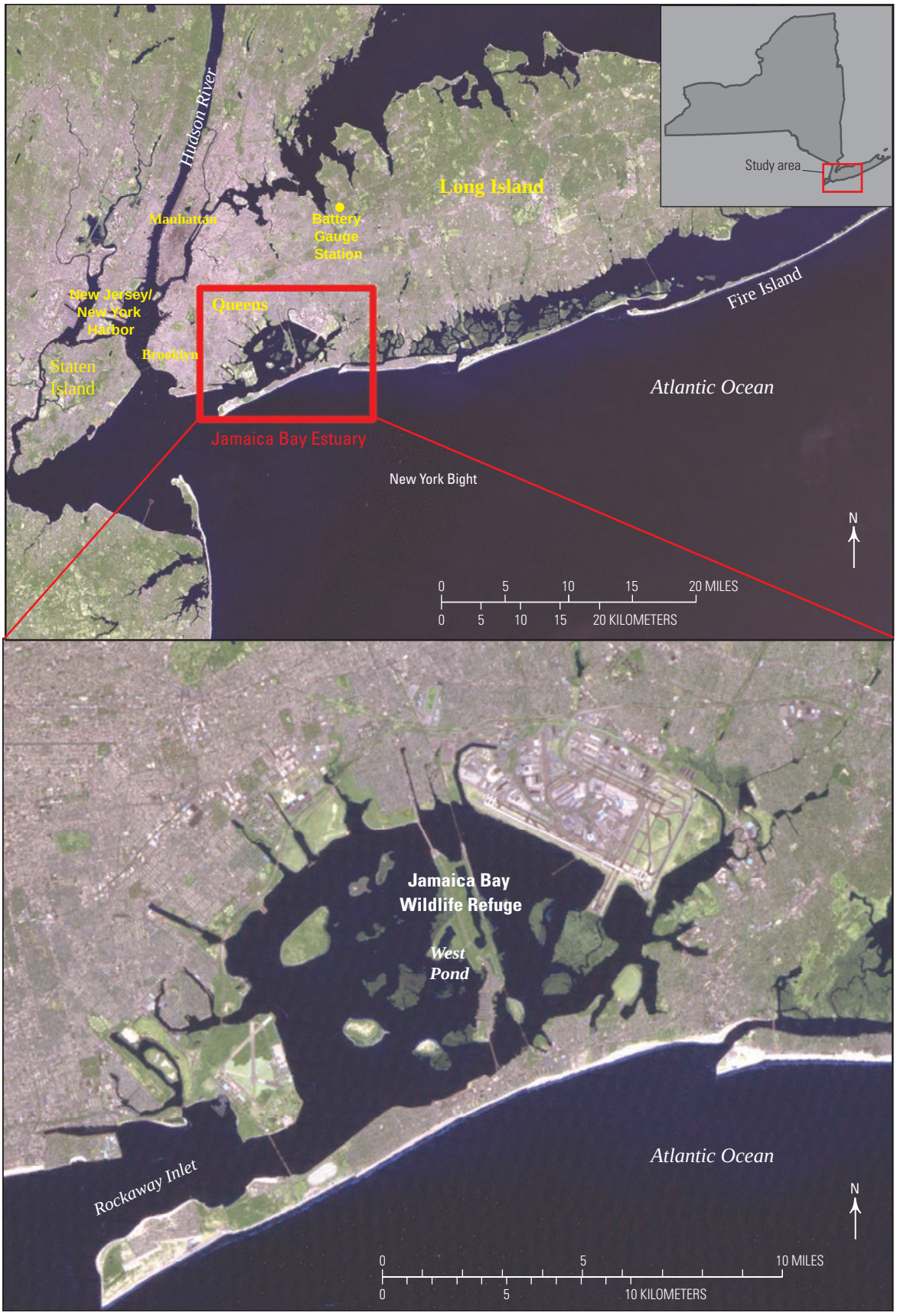

Figure 1. Location of Jamaica Bay estuary, New York City.

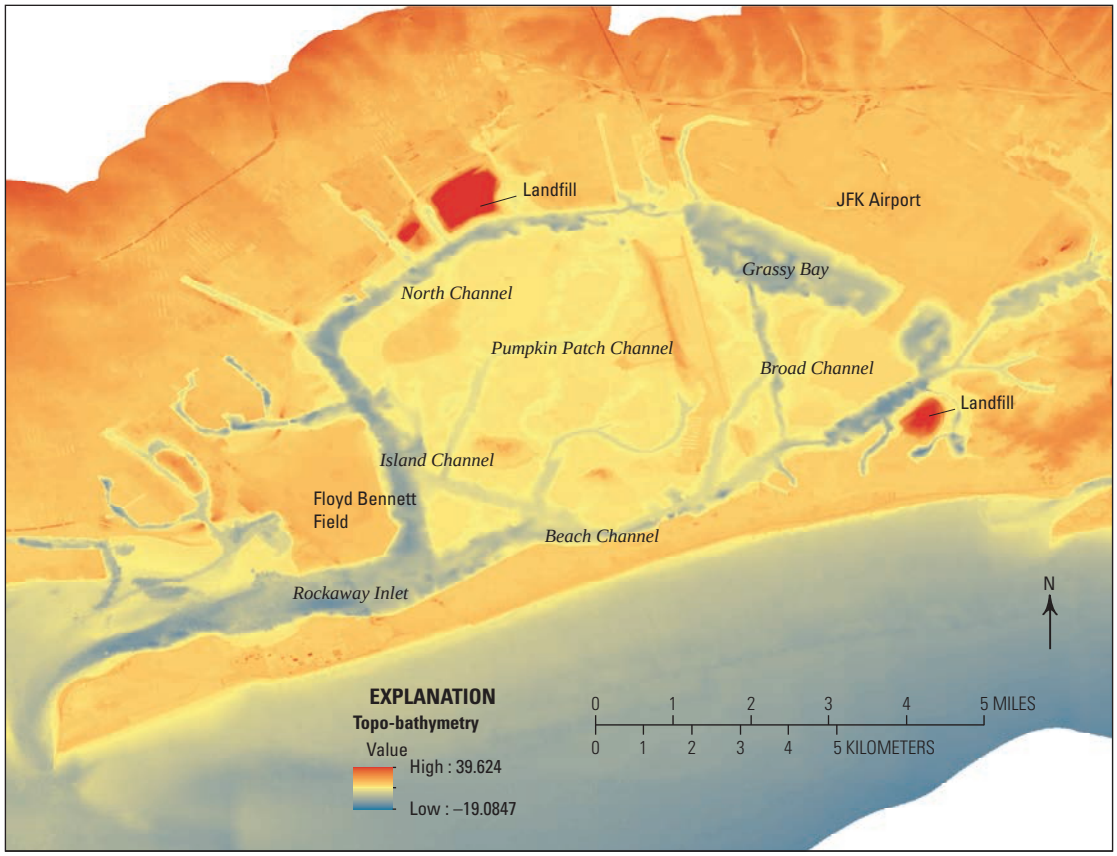

Figure 2. Navigational system in Jamaica Bay, New York City.

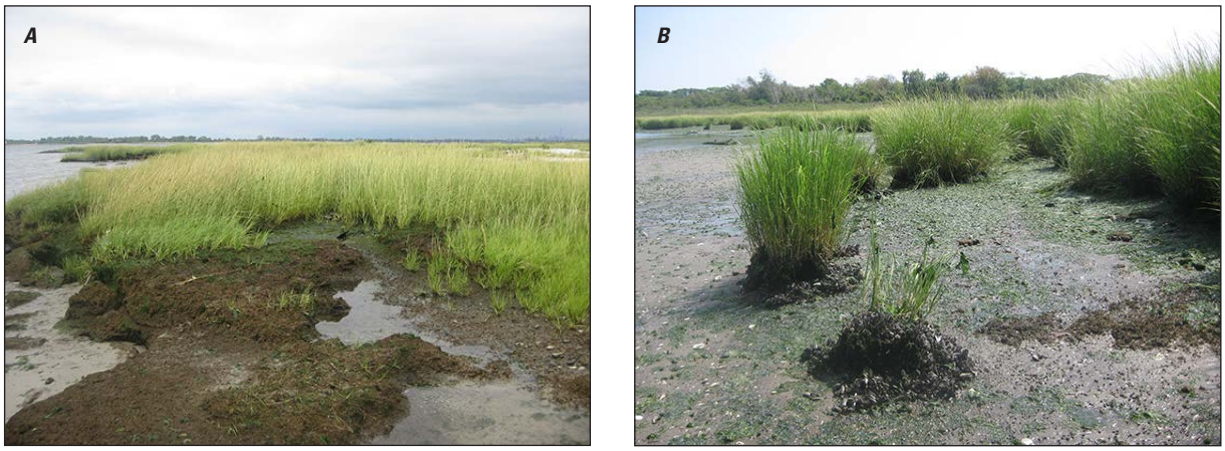

Photographs by Hongqing Wang, U.S. Geological Survey

Figure 3. *A*, Marsh deterioration by edge erosion down to the underlying mineral sediment at Ruffle Bar, and *B*, marsh fragmentation and conversion to mudflat caused by erosion at Four Sparrow in Jamaica Bay, New York City.

Changes in the bay's elevation contours by the westward progression (about 1.4 km) of the Rockaway Peninsula between the mid-1800s to the 1930s, the dredging of navigational channels, the stabilization of Rockaway Inlet, landfills, armoring of the shoreline periphery, and the construction of John F. Kennedy International (JFK) Airport in early 1940s with its runway into the bay have reduced sediment transport or affected water circulation (Black, 1981; Swanson and Wilson, 2008; Renfro, 2010; Talke and others, 2014). The tributaries, basins, tidal creeks, and canals within Jamaica Bay have also been highly altered over the years and tend to have little or no freshwater flow aside from the combined sewer outfalls. Borrow pits, other areas such as Grassy Bay (fig. 2) from which sandy sediment was dredged to construct JFK Airport, and deep navigation channels may be acting as sediment sinks (Swanson and Wilson, 2008). Historical evidence indicates that prior to 1900 the bay was a weakly ebb-dominated system, while in present day, the bay is a flood-dominated system (e.g., Swanson and Wilson, 2008). The increased wave energy and sediment flushing time caused by the deeper average depths after construction may affect sediment accretion. There is also the possibility that nitrogen-enriched water is causing an excessive growth of sea lettuce (*Ulva lactuca* L.), which is carpeting the bay's bottom and mudflat (fig. 3) and preventing sediments from being resuspended into the water for redistribution onto the marsh surfaces (Hartig and others, 2002; Wigard and others, 2014). The substantial marsh loss that is already occurring implies that accretion rates in Jamaica Bay may be insufficient, even at present rates of sea-level rise (SLR), to compensate for losses due to erosion and other factors (Hartig and others, 2002).

Coastal ecosystem evolution and resilience under climate change, SLR, and increased frequency and intensity of hurricanes and storms depend on sufficient vertical accretion and wetland mass continuity (Cahoon, 2006; Turner and others, 2006; Wigand and others, 2014; Miselis and others, 2015). The fundamental material for such accretion and wetland mass continuity is sufficient mineral sediment supply, delivery, and deposition onto wetland surface for the plants to colonize and to allow for the vegetation community to evolve. Therefore, sediment management is a major component of marsh restoration in Jamaica Bay to mitigate wetland loss. Nevertheless, it is still unclear whether or not Jamaica Bay salt marshes can be self-sustaining in the long run in the face of projected climate change, SLR, hurricanes and storms, eutrophication, and inadequate sediment supply to the marsh surface. Any activities related with sediment movement onto salt marshes in Jamaica Bay will play a critical role in the resilience and sustainability of the bay because marsh resilience is strongly related to sediment supply (Fagherazzi and others, 2013b).

Hurricane Sandy

Large-scale storm events may be an important component in sediment transport processes and marsh surface accumulation, especially for coasts under sediment-poor, sand-starved, and low energy conditions (Goodbred and Hine, 1995; Cahoon, 2006). Hurricane Sandy provides a critical opportunity for studying the effects of hurricanes on short-term sedimentation and erosion and long-term morphologic changes in the salt marshes of Jamaica Bay. Hurricane Sandy was an extreme storm (1,850 km in diameter, three times of the size of Hurricane Katrina in 2005) with a long return interval (about 700 years for path and about 100 years for magnitude of flooding) (Blake and others, 2013; Sopkin and others, 2014). A new analysis indicates that Hurricane Sandy was the largest hurricane at New York Harbor (fig. 1) since at least 1700 with a return period of 260 (170–420) years for flood (Orton and others, 2016). Hurricane Sandy made landfall at 23:30 Coordinated Universal Time (UTC; timed with the full-moon high tide) near Brigantine, New Jersey, approximately 130 km southwest of Jamaica Bay (fig. 4), on October 29, 2012, with maximum sustained winds of 130 kilometers per hour (kph) and a central pressure of 945 millibars (mb), delivering hurricane-force winds and storm tides (e.g., 3.4 m above 2012 mean sea level [MSL] at the Battery gage station, NY, fig. 1) (Brandon and others, 2014). Hurricane Sandy caused severe flooding along portions of the northeast coast, including 1,132 km^2 of New York City (Orton and others, 2015a), and breaches across barrier islands in New Jersey and New York such as Fire Island (fig. 1) (Sopkin and others, 2014). East and West Ponds, two freshwater ponds within the JBWR (fig. 1), were breached by Hurricane Sandy storm surge and waves and were inundated with saltwater (American Littoral Society, 2012). Consequently, the land that formerly stood between the ponds and Jamaica Bay, including part of the loop trail around West Pond, was washed away. More importantly, the breaches have transformed the ponds entirely, and rendered them unable to support the species that depended upon them for freshwater.

Previous Studies

Hurricanes and tropical cyclones are among the important driving forces that reshape coastal landscape quickly and affect long-term estuary resilience and sustainability through their long-term impact on coastal wetland morphology (Cahoon and others, 1995; Nyman and others, 1995; Cahoon, 2006). They can directly affect soil elevation by sediment deposition, erosion, compaction, soil water flux (shrink and swell), and lateral tearing and folding of vegetated substrate. The end result can be conversion of marshes into mudflats or even into open water, or increased vegetation mortality can be caused by increased salinity exceeding the vegetation's threshold of salt tolerance as a result of saltwater intrusion (Cahoon, 2006). On the contrary, storms can also deliver enough sediment to raise soil surface elevation and stimulate organic matter production, thus helping coastal wetlands to survive rising sea level and subsidence (Chmura and Kosters, 1994; Cahoon, 2006; Turner and others, 2006; Tweel and Turner, 2012). The effect of major hurricanes on sediment

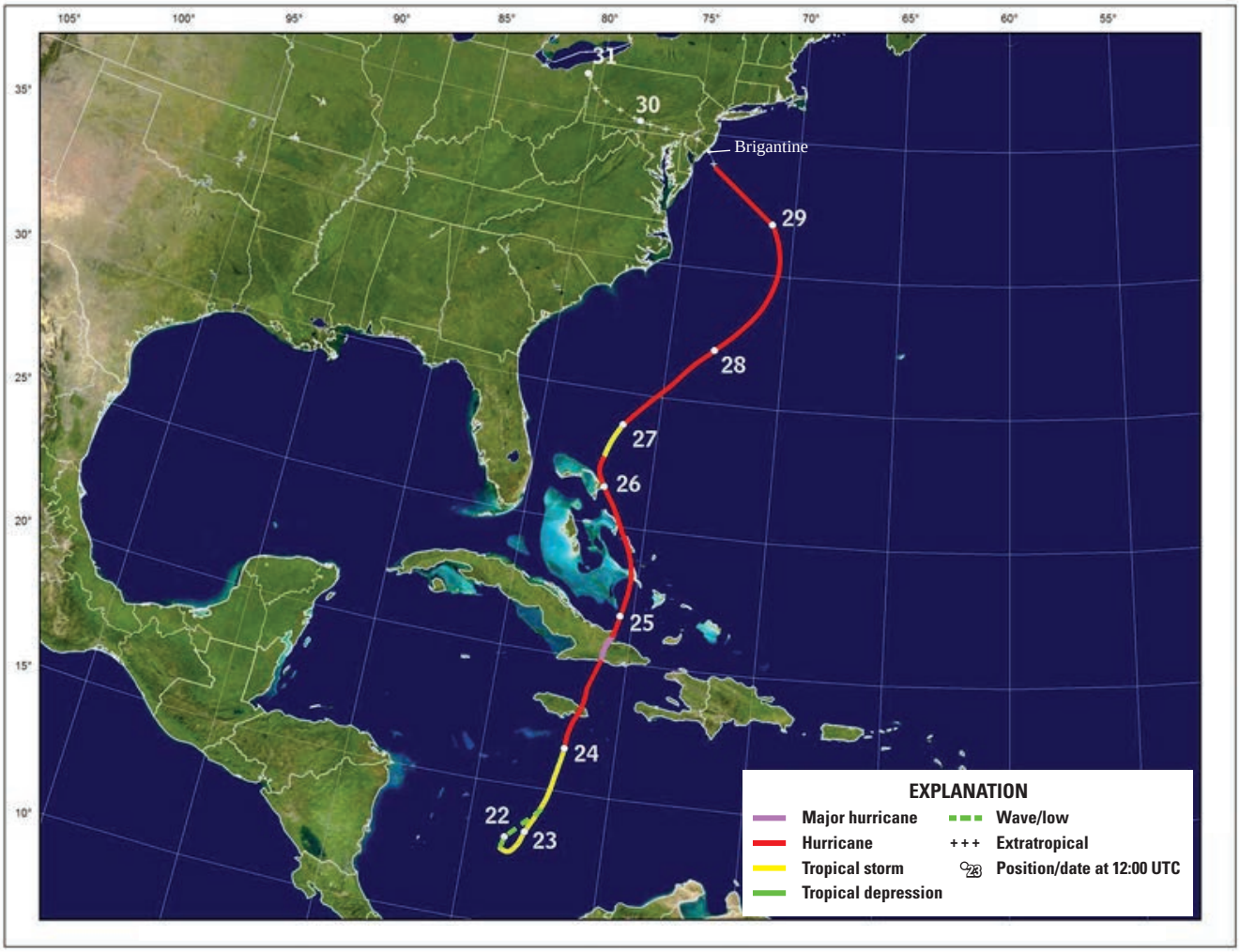

Base from Blake and others, 2013

Figure 4. Track of Hurricane Sandy during October 22–29, 2012, and landfall on October 30, 2012, along the northeast coast (source: Blake and others, 2013).

accumulation can be detected by identifying the coincidence of cesium-137 (^{137}Cs) and lead-210 (^{210}Pb) activity peaks with mineral peaks, indicating that although storm-induced sediment may become reworked by physical or biological processes, some of the storm-induced sediment is indeed retained and incorporated into the long-term sediment accumulation for maintaining surface elevation (Chmura and Kosters, 1994). The thickness of newly deposited mud on Louisiana's coastal wetlands during Hurricane Katrina was 5.18 ± 7.7 centimeters (cm; range: 0–68 cm) (Turner and others, 2006; McKee and Cherry, 2009). A single hurricane deposit may be the equivalent of over a century of nonstorm-surge sedimentation in coastal Louisiana's wetlands (Williams and Flanagan, 2009). In coastal Louisiana, it was estimated that the long-term hurricane sedimentation rate is about 0.24 centimeter per year (cm/yr), approximately 25 percent of the total long-term vertical accretion rate (Nyman and others, 1995). In the Chenier Plains west of coastal Louisiana, Hurricane Rita (2005) may have contributed 27–66 percent of the long-term sedimentation, based on the estimated recurrence interval of large hurricanes (Williams and Flannagan, 2009). Hurricanes can simultaneously influence surface and subsurface soil processes where the net outcome of soil elevation is not always predictable solely from the observed effects of sediment deposition and erosion. This influence of large storms on subsurface processes appears to be the single most important difference between high frequency, low magnitude cold fronts or winter storms and low frequency, high magnitude hurricanes (Cahoon and others, 1995). The greatest impact on erosion and deposition in coastal wetlands could be caused by hurricane-force winds (greater than or equal to 74 miles per hour [mph]), not by the passage of winter fronts (Chmura and Kosters, 1994).

No field observations on sediment deposition and erosion due to Hurricane Sandy were reported for wetlands along the New Jersey or New York coasts. Nevertheless, evidence of Hurricane Sandy-induced sediment deposition/erosion has been provided for other types of coastal systems. For example, deposition associated with Hurricane Sandy (5–20 cm) was

found from four cores extracted from Seguine Pond (about 1.2 m back barrier) on the southern coast of Staten Island (fig. 1), New York (Brandon and others, 2014). It was reported that little measurable morphological change in Barnegat Bay was caused by Hurricane Sandy along the southern New Jersey coast even though the barrier shoreline retreated by 12 m during the storm (Miselis and others, 2015). Miselis and others (2015) found that within the estuary near Mantoloking, north of the Barnegat Bay, the storm resulted in about 250 cubic kilometers (km^3) of deposition and about 50 km^3 of erosion within the bay with measurable changes of ±35 cm, but this was localized and not widespread. A study using glider observations and the regional ocean modeling system (ROMS) found that a substantial portion of the bed in the inner continental shelf along the New Jersey and New York coasts was likely eroded from the northern New Jersey shelf north of the Hurricane Sandy track and deposited along the southern portion of the shelf (Miles and others, 2015).

Sediment from hurricanes varies spatially (uneven thickness or spatial discontinuity) depending on the characteristics of the hurricanes (for example, storm track, wind speed, areal extent, and forward speed), location relative to hurricane path, and local bathymetry and channel morphology (Chmura and Kosters, 1994; Turner and others, 2006; Williams and Flanagan, 2009; Tweel and Turner, 2012). Normally, more storm-generated sediment deposition was found at areas closer to the storm track and with a higher bulk density in the top surface layer, a higher mineral content, and coarser grain size compared to pre-storm condition or sites far away from the storm track (Cahoon and others, 1995; Turner and others, 2006; McKee and Cherry, 2009; Tweel and Turner, 2012). Hurricane sediment deposition thickness on marsh surfaces can extend several hundred meters from the tidal creek banks and shore edge, and decreases with distance into the marsh (Goodbred and Hine, 1995; McKee and Cherry, 2009). Generally, the overlying storm surge sediment in wetland soils is coarser than the pre-storm surge sediment with a lower organic content and the presence of offshore foraminiferal microfossils; therefore, the boundary can be readily identified in the field and through grain size analysis (Turner and others, 2006; Miselis and others, 2015; Smith and others, 2015).

In a general sense, hurricanes have the potential to mobilize and transport sediments across the coastal landscape as a function of increasing storm energy. Tidal, estuarine, and wind-driven currents can then redistribute suspended sediments, ultimately leading to deposition in the deeper waters of the bay, and, possibly, in salt marshes. Despite the recognition of spatial variability in storm-generated sediment deposition and erosion across coastal landscapes from field observations and marsh core sampling as well as geochronological analysis, little is known about the mechanism (specific physical and biological processes and controlling factors) on such spatial variability in hurricane-induced sedimentation and associated wetland morphological dynamics. At present, the capability of quantifying and predicting erosion, sediment transport, and deposition in wetlands with vegetation during extreme events remains very limited.

Numerical models that couple physical and ecological processes involved in hurricanes and tropical cyclones can be powerful tools to detect and predict the spatial estuarine and wetland morphological spatial response to hurricane/storm disturbances (Hu and others, 2015; Liu and others, 2015; Miles and others, 2015; Xu and others, 2015). In order to simulate hurricane effects on wetland morphological change, physical processes, including hurricane winds, waves, storm surge, sediment transport, and morphological dynamics, need to be incorporated into the modeling system. Such modeling efforts have been tested for coastal areas, including storm-generated morphological changes in offshore shallow areas (Bentley and others, 2002; Miles and others, 2015; Xu and others, 2015), low-lying barrier islands (Lindemer and others, 2010), and beaches and dunes (Stockdon and others, 2007). However, there are few such studies on wetland spatially-explicit morphological change under the influences of hurricanes and extratropical storms in spite of the observed hurricane-induced sediment deposition on wetland surface (Nyman and others, 1995; Cahoon, 2006; Turner and others, 2006) and evidence of preservation of hurricane sediment in wetland soils (Smith and others, 2015). The lack of modeling hurricane-induced sediment movement in coastal wetlands greatly limits the capability to predict wetland morphologic change under the increased impacts of storms due to climate change. Furthermore, the interactions between wetland vegetation and these physical processes need to be explored and quantified in order to detect wetland responses to hurricanes. For example, previous field and modeling studies show that the magnitude of vegetation-generated flow resistance, storm surge reduction, wave attenuation, bed shear stress, and associated sediment delivery, deposition, and erosion vary with the vegetation's physical characteristics (stem height, density, diameter, and flexibility) (Temmerman and others, 2005; Loder and others, 2009; Nardin and Edmonds, 2014; Zhao and Chen, 2014, 2016; Chen and others, 2016). However, no studies have examined hurricane effects on the spatial patterns and changes in sediment movement and wetland morphology across salt marshes in Jamaica Bay using a fully dynamic numerical modeling approach. This integrated modeling and field investigation is important in that it provides quantitative information about wetland morphologic dynamics in the salt marshes of Jamaica Bay under future predicted climate change-induced accelerated SLR and hurricanes or storms of increased frequency and intensity so that proactive management and restoration can be planned and evaluated.

Purpose and Scope

The specific objectives of this project are to (1) develop an integrated high-resolution numerical modeling system that couples winds, waves, storm surge, sediment transport, and wetland morphologic dynamics by incorporating new parameterizations of momentum and energy dissipation caused by the salt marshes, (2) determine the magnitude and understand the

mechanism of sediment movement onto salt marshes by Hurricane Sandy and its short-term (event and 1 year) and long-term (multiple years and decadal) effects on spatial wetland morphological changes across Jamaica Bay, and (3) predict the effects of potential future hurricanes on spatial sediment deposition, erosion, and marsh morphology in Jamaica Bay. Some specific issues will be addressed in this study: (1) the magnitude and spatial patterns in Hurricane Sandy-induced sediment deposition and erosion in Jamaica Bay and associated salt marsh islands; (2) the sources of Sandy-induced sedimentation on wetlands; (3) the driving forces for hurricane-induced wetland morphological changes; and (4) the role of saltmarsh vegetation on sediment transport, deposition, and erosion in Jamaica Bay.

This field observation and process-based numerical modeling integrated study may be helpful to the NPS-GNRA, New York City Department of Parks & Recreation, U.S. Army Corps of Engineers (USACE), and other interested parties in support of their decisionmaking process. This study is of great importance for the best management of saltmarsh protection and restoration activities under climate change, SLR, and increased frequency and intensity of hurricanes and tropical storms to mitigate the loss of wetlands and associated ecosystem services not only in Jamaica Bay, but also wetlands in other Northeast Atlantic coastal regions.

Methods

The process-based numerical model package, the Delft3D model (Deltares, 2017) was used to develop the hurricane-wetland morphology model and to simulate the effects of Hurricane Sandy and potential future hurricanes on spatial patterns of sediment deposition and erosion and associated wetland morphological change in salt marshes of Jamaica Bay. The theory and governing equations of the wind, waves, storm surge, sediment transport models and their coupling to detect salt marsh morphological change are described in more detail in the section "Modeling System." The nested computational model domains, model parameters, and initial and boundary conditions are described in the section of "Model Setup." Afterward, the methodologies of model calibration and validation, long-term simulations, and design of hypothetical hurricanes are also described in detail.

Modeling System

The Delft3D model suite has had international application, and is capable of simulating flow, sediment transport, waves, water quality, morphological changes, and ecological processes in coastal, riverine, and estuarine environments (Lesser and others, 2004; Temmerman and others, 2005; Hu and others, 2009, 2015; George and others, 2012). The model suite consists of several modules that can interact with each other, including flow, waves, sediment transport, water quality, and morphology. In this study, hurricane winds, waves, storm surge, and sediment transport processes were integrated into a coupled modeling system for the development of the hurricane-wetland morphology model for the Jamaica Bay wetlands (fig. 5).

Wind Model

To simulate the effects of hurricanes on wetland morphology, hurricane wind fields need to be captured; however, the Delft3D model did not contain a wind module that could reasonably capture wind fields during large, complex hurricanes. Therefore, an improved asymmetric Holland-type vortex wind

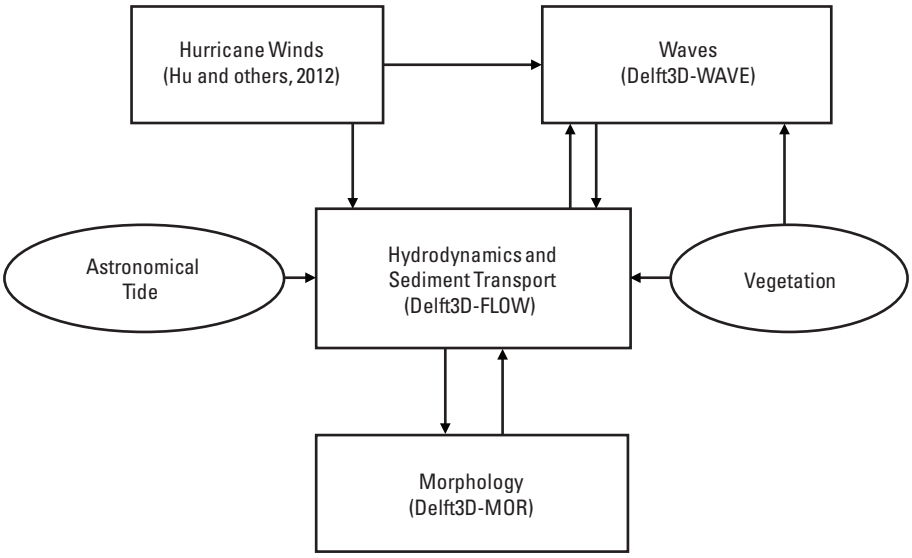

Figure 5. Structure of the morphology modeling system for Jamaica Bay, which couples wind, waves, storm surge, and sediment transport.

model (Hu and others, 2012) was used to generate surface wind fields by Hurricane Sandy and future potential hurricanes over the large geographic domain covering Cape May, Long Island, Nantucket Island, and New York Bight. Three improvements have been made to retain consistency between the input parameters and the model output and to better resolve the asymmetric structure of the hurricane. First, to determine the shape parameter in the Holland-type wind model, the Coriolis effect was included and the range restriction was removed. Second, the effect of the translational velocity of the hurricane was excluded from the input of specified wind speeds before applying the Holland-type vortex to avoid exaggeration of the wind asymmetry. Third, a new method was introduced to develop a weighted composite wind field that makes full use of all the wind field parameters. The wind model creates a two-dimensional surface wind field based on the National Hurricane Center (NHC) Automated Tropical Cyclone Forecasting (ATCF) best track data (ftp://ftp.nhc.noaa.gov/atcf/archive/). The simulated wind fields were used to force hurricane waves and storm surges.

Wave Model

Wind-generated waves produce bottom shear stresses important to sediment resuspension in shallow and vegetated areas. The SWAN (Simulating WAves Nearshore) model was used to compute storm-generated wave parameters including significant wave height, peak period, and direction of the wave field at each grid point in order to compute wave-current combined bottom shear stress. The SWAN model solves the spectral wave action balance equation without inferred restrictions on the spectrum for the evolution of wave growth. This equation represents the effects of wave propagation, refraction, shoaling, generation, dissipation, and nonlinear wave-wave interactions. In Cartesian coordinates, the governing equation can be expressed as:

$$\frac{\partial}{\partial t}N+\frac{\partial}{\partial x}c_x N+\frac{\partial}{\partial y}c_y N+\frac{\partial}{\partial \sigma}c_\sigma N+\frac{\partial}{\partial \theta}c_\theta N=\frac{S}{\sigma} \quad (1)$$

where

N is action density,

c_x and c_y are the propagation velocities of wave energy in spatial x-, y-space,

c_σ and c_θ are the propagation velocities in spectral space σ-, θ-space, and

S is the source term in terms of energy density representing the effects of wave generation, dissipation, and nonlinear wave-wave interactions.

The first term on the left-hand side of this equation represents the local rate of change of wave action density in time, the second and third term represent propagation of wave action in geographical space (with propagation velocities c_x and c_y in the x- and y-dimension, respectively). The fourth term represents shifting of the relative frequency due to variations in depths and currents (with propagation velocity c_σ in the σ-space). The fifth term represents depth-induced and current-induced refraction (with propagation velocity c_θ in the θ-space). The expressions for these propagation speeds are taken from the linear wave theory.

Wave dissipation due to vegetation, as one of the source terms, is based on the cylinder approach of Dalrymple and others (1984). Mendez and Losada (2004) extended this approach for irregular waves. The expression of vegetation-induced wave dissipation term is expressed by the following equation:

$$S_{ds,veg}=-\sqrt{\frac{2}{\pi}}g^2\tilde{C}_D b_v N_v\left(\frac{\tilde{k}}{\tilde{\sigma}}\right)^3\frac{sinh^3\tilde{k}\alpha h+3sinh\tilde{k}\alpha h}{3kcosh^3\tilde{k}h}\sqrt{E_{tot}}E(\sigma,\theta) \quad (2)$$

where

g is gravitational acceleration,

$\tilde{C}_D$ is the bulk drag coefficient,

b_v is the stem diameter of plant,

N_v is the number of plants per square meter,

k is the wave number,

$\tilde{k}$ is the mean wave number,

$\tilde{\sigma}$ is the mean angular frequency,

αh is the effective vegetation stem height,

$E(\sigma,\theta)$ is the energy density, and

E_{tot} is the total energy.

The current version of the Delft3D suite has a limitation that only one type of vegetation can be included in the wave module. In this study, a representative set of vegetation parameters (average values for low marsh and high marsh, refer to "Model Parameters") were chosen for the study area.

Flow Model

The wind and wave models were coupled with the hydrodynamic model in Delft3D (Delft3D-FLOW) to hindcast waves and storm surge caused by Hurricane Sandy and future potential hurricanes. The Delft3D-FLOW model computes flow characteristics (water depth, flow velocities and directions, turbulence characteristics). The effects of vegetation on flow characteristics were represented by considering the influence of the plant structures on drag and turbulence. The coupled model has been successfully applied to the simulations of storm surge height and water levels of Hurricanes Katrina (2005), Gustav (2008), and Isaac (2012) along the Gulf Coast (Chen and others, 2008; Dietrich and others, 2011; Hu and other, 2015). Although the coupled model was focused on the northeastern Gulf of Mexico, the generally good model/observation agreement has demonstrated the effectiveness of the integrative approach to wave and surge predictions in a complex coastal environment, including Jamaica Bay along the North Atlantic coast.

The main component of the Delft3D model, Delft3D-FLOW, is a multi-dimensional (2D or 3D) hydrodynamic (and transport) simulation program that solves the Navier-Stokes

equations for an incompressible flow, under the shallow water and the Boussinesq assumptions, and computes sediment transport and updates morphology simultaneously with the flow. The vertically integrated governing equations in a Cartesian coordinate (x, y) are

$$\frac{\partial \zeta}{\partial t} + \frac{\partial\left[(d+\zeta)u\right]}{\partial x} + \frac{\partial\left[(d+\zeta)v\right]}{\partial y} = Q \tag{3}$$

$$\frac{\partial u}{\partial t} + u\frac{\partial u}{\partial x} + v\frac{\partial u}{\partial y} + fv = \frac{-P_x}{\rho_0} + F_x + M_x \tag{4}$$

$$\frac{\partial v}{\partial t} + u\frac{\partial v}{\partial x} + v\frac{\partial v}{\partial y} - fu = \frac{-P_y}{\rho_0} + F_y + M_y \tag{5}$$

where

t is time,

d is the local water depth,

ζ is the free-surface elevation above mean sea level,

u and v are depth-averaged velocity in the x or y direction,

Q is the discharge or withdrawal of water, precipitation, and evaporation,

f is the Coriolis coefficient,

P_x and P_y are the pressure gradient,

F_x and F_y are the turbulent momentum flux in the x or y direction, and

M_x and M_y represent other source and sink terms in the momentum equations including the free-surface wind stress, bottom shear stress under currents and waves, wave radiation stress, and vegetation-induced drag.

Vegetation plays a unique role in coastal protection by attenuating strong winds, waves, and storm surge. In our model, the flow resistance caused by vegetation drag was modeled as sink terms, $\frac{-1}{2}\lambda u\sqrt{u^2+v^2}$ and $\frac{-1}{2}\lambda v\sqrt{u^2+v^2}$, in the momentum equations, and it was strictly separated from the bed friction itself (without vegetation) to avoid unrealistic exaggeration of bed shear stress for sediment transport (Baptist, 2005). For submerged vegetation,

$$\lambda = C_D b_v N_v \tag{6}$$

For nonsubmerged vegetation,

$$\lambda = C_D b_v N_v \frac{h_v}{h}\frac{C_b^2}{C^2} \tag{7}$$

$$C = C_b + \frac{\sqrt{g}}{K} ln\left(\frac{h}{h_v}\right)\sqrt{1+\frac{C_D b_v N_v h_v C_b^2}{2g}} \tag{8}$$

where

C_D is the vegetation drag coefficient,

C_b is the roughness of the bed without vegetation,

h and h_v are the local water depth and vegetation height, respectively, and

K is the von Karman constant.

Two approaches are available to represent wetland vegetation in the Delft3D-FLOW and SWAN models. The first approach uses an enhanced Manning's roughness coefficient that is spatially assigned according to land-cover classes. The second approach treats vegetation as a series of rigid cylindrical structures described by vegetation parameters, such as stem height and diameter, and population density. In Delft3D-FLOW, the trachytopes (roughness) functionality is used to consider vegetation effects with the second approach. This functionality allows the user to specify the bed roughness on a sub-grid level by defining and using various land use or roughness/resistance classes. The first approach can only roughly distinguish different types of wetland (for example, woody wetland and herbaceous wetland) and is usually applied to large-scale simulations. For example, according to the USGS National Land Cover Database (NLCD) in 1992 (Vogelmann and others, 2001), the Manning's coefficient values are 0.02, 0.55, and 0.11 for open water, woody wetlands, and herbaceous wetlands, respectively (Bunya and others, 2010). Subsequent research indicates friction coefficients of about 0.4 for wetlands (Wang and others, 2007). The second approach deals with detailed vegetation parameters and can be applied to small-scale simulations to probe the effects of vegetation with various specific biophysical characteristics such as stem height and density. Both approaches were employed in this study. In the ocean-scale and regional domains, the first approach with Manning's coefficients was used (see tables 3–5 in Bunya and others [2010] for Manning's n values associated with different land-cover classes), while in the local and bay-wide domains, the second approach with trachytopes was used to account for vegetation effects.

Coupling of Flow Model and Wave Model

The flow model (Delft3D-FLOW) provides water levels and currents to the wave model (Delft3D-WAVE or SWAN). The wave model provides wave parameters to the flow model for calculations of radiation stresses and combined wave-current bed shear stresses. The time step for the flow model is 3–360 seconds, depending on domain resolutions; the time step for the wave model is 1 hour. The two models provide updated simulation results to each other every hour. The bed shear stress caused by the combination of waves and a current ($\dot{\tau}_{cw}$) is enhanced beyond the value which would result from a

linear addition of the bed shear stress due to waves, $\acute{\tau}_w$, and the bed shear stress due to a current, $\acute{\tau}_c$. Various, often very complex, methods exist to describe the bottom boundary layer under the combined current and wave action and the resulting virtual roughness.

Sediment Transport and Morphology Model

The sediment transport model (embedded in Delft3D-FLOW) and morphology model (Delft3D-MOR) in Delft3D, coupled with the flow model, were used to simulate a sequence of sediment transport, suspension, erosion, and deposition in Jamaica Bay caused by Hurricane Sandy and the hypothetical hurricanes. The sediment model computes suspended sediment concentrations and sedimentation/erosion rates at each time step and each grid cell on the basis of the 3D advection-diffusion equation for suspended sediments (Lesser and others, 2004; Hu and others, 2009; George and others, 2012; Liu and others, 2015). Most of the sediment is eroded and resuspended from the channel bottom and banks, where the velocities are high and vegetation does not protect the substrate. Therefore, erosion at the mudflat-marsh edge by waves was explored with wind, waves, tides (for example, flood and ebb flows), velocity, and vegetation characteristics. For sediment transport, velocity and turbulence results from the hydrodynamics model were used to calculate the advection and diffusion of the sediment. The resulting concentration and new distribution of the sediment were then incorporated into the hydrodynamic model, and the velocity and turbulence were recalculated. This feedback cycle was repeated for the duration of each simulation.

In the sediment model, the transport of suspended sediment is governed by the advection-diffusion equation:

$$\frac{\partial c}{\partial t}+\frac{\partial uc}{\partial x}+\frac{\partial vc}{\partial y}+\frac{\partial\left(w-w_s\right)c}{\partial z}-\frac{\partial}{\partial x}\left(\varepsilon_x\frac{\partial c}{\partial x}\right)-\frac{\partial}{\partial y}\left(\varepsilon_y\frac{\partial c}{\partial \eta}\right)-\frac{\partial}{\partial z}\left(\varepsilon_z\frac{\partial c}{\partial z}\right)=0 \quad (9)$$

where

c is mass concentration of a certain sediment fraction;

u, v, and w are flow velocity components;

ε_x, ε_y, and ε_z are the eddy diffusivities of sediment fraction; and

w_s is the sediment setting velocity of the sediment fraction.

At the water surface boundary, the vertical flux through the free surface is set to zero, which is

$$-w_s c-\varepsilon_z\frac{\partial c}{\partial z}=0, \text{at } z=\zeta \quad (10)$$

where $z=\zeta$ is the location of the free surface.

For cohesive sediment fraction (mud), the settling velocity is set at $5*10^{-4}$ meters per second (m/s; table 3). For noncohesive sediment fraction (sand), the settling velocity is calculated from sediment diameter by using the formula by Van Rijn (1993):

$$w_s=\begin{cases}\dfrac{\left(s-1\right)gD_s}{18\mu} & \text{if } 65\ \mu\text{m}<D_s\ \le\ 100\ \mu\text{m}\\ \dfrac{10\mu}{D_s}\left(\sqrt{1+\dfrac{0.01\left(s-1\right)gD_s^3}{\mu^2}}-1\right) & \text{if } 100\ \mu\text{m}<D_s\ \le\ 1{,}000\ \mu\text{m}\\ 1.1\sqrt{\left(s-1\right)gD_s} & \text{if } 1{,}000\ \mu\text{m}<D_s\end{cases} \quad (11)$$

where

s is the sediment relative density ρ_s/ρ_w;

D_s is the representative diameter; and

μ is the kinematic viscosity coefficient of water, in square meters per second.

The exchange of material in suspension and the bed is modeled by calculating the sediment fluxes from the bottom computational layer to the bed, and vice versa. The boundary condition at the bed is given by

$$-w_s c-\varepsilon_z\frac{\partial c}{\partial z}=D-E, \text{at } z=z_b \quad (12)$$

where D and E are the sediment deposition and erosion flux (in kilograms per square meter per second) of sediment fraction, respectively. For the erosion and deposition of mud on the bed, the Partheniades-Krone approach (Partheniades, 1965) was used:

$$E=M_s\times S\left(\tau_{cw},\tau_{cr,e}\right) \quad (13)$$

$$D=w_s\times c_b\times S\left(\tau_{cw},\tau_{cr,d}\right) \quad (14)$$

$$c_b=c\left(z=\frac{z_b}{2},t\right) \quad (15)$$

where

M_s represents the erosion parameter (in kilograms per square meter per second);

$S\left(\tau_{cw},\tau_{cr,e}\right)$ is the erosion step function which is equal to $\left(\dfrac{\tau_{cw}}{\tau_{cr,e}}-1\right)$ when $\tau_{cw}>\tau_{cr,e}$ and 0 when $\tau_{cw}\le\tau_{cr,e}$;

c_b is the average sediment concentration in the near bottom computational layer;

$S(\tau_{cw}, \tau_{cr,d})$ is the deposition step function which is equal to $\left(1-\frac{\tau_{cw}}{\tau_{cr,d}}\right)$ when $\tau_{cw} > \tau_{cr,e}$ and 0 when $\tau_{cw} \geq \tau_{cr,d}$; and

$\tau_{cr,e}$ and $\tau_{cr,d}$ are the critical erosion and deposition shear stress, respectively.

For sand, the method in Van Rijn and others (2000) was followed. Erosion and deposition fluxes are evaluated at the so-called kmx-layer, which is defined entirely above Van Rijn's reference height *a* (Van Rijn, 1993). The erosion and deposition fluxes are given as follows:

$$E = \alpha_2 \varepsilon_s \left(\frac{c_a - c_{kmx}}{\Delta z}\right) \tag{16}$$

$$D = \alpha_1 c_{kmx} w_s \tag{17}$$

where

α_1 and α_2 are the correction factors;

ε_s is the sediment diffusion coefficient at the bottom of the kmx cell;

c_a is the reference concentration;

c_{kmx} is the average concentration at the kmx cell; and

Δz is the difference between the center of the kmx cell and Van Rijn's reference height, $\Delta z = z_{kmx} - a$.

The bedload transport of noncohesive sediment has taken the formula by Van Rijn (1993). Van Rijn (1993) distinguished between sediment transport below the reference height *a*, which is treated as bedload transport, and sediment transport above the reference height, which is treated as suspended load. Using an approximation method developed by Van Rijn and others (2003), the magnitude of the bedload transport is

$$|S_b| = 0.006 \rho_s w_s D_{50} M^{0.5} M_e^{0.7} \tag{18}$$

where

S_b is the bedload transport (in kilograms per meter per second),

ρ_s is the sediment density,

D_{50} is the median grain diameter,

M is the sediment mobility number due to waves and currents,

M_e is the excess sediment mobility number, and

$$M = \frac{v_R^2 + U_{orb}^2}{(s-1) g D_{50}} \tag{19}$$

$$M_e = \frac{\left(\sqrt{v_R^2 + U_{orb}^2} - v_{cr}\right)^2}{(s-1) g D_{50}} \tag{20}$$

where

v_{cr} is the critical depth-averaged velocity for initiation of motion (based on the Shields curve);

v_R is the magnitude of an equivalent depth-averaged velocity computed from the velocity in the bottom computational layer, assuming a logarithmic velocity profile; and

U_{orb} is the wave near-bed, peak orbital velocity.

The morphological change is the sum of the changes caused by suspended loads and bedloads. Normally, repeated inputs representing normal or abnormal physical conditions from field measurements are used in model coupling for long-term simulations (De Vriend and others, 1993). Boundary condition inputs, such as time series of tides, winds, waves, and mass fluxes, cannot be specified for a decadal or longer time span because of the lack of field measurements. In reality, even if detailed field measurements of these time series of boundary conditions were available, it would be extremely time consuming for high-resolution process-based models to simulate decadal-scale wetland morphologic dynamics. To reduce computational costs in simulations of long-term wetland morphological changes, a morphological acceleration factor, fMOR, was applied to calculate/update long-term bathymetric change and coastline change from the real-time calculation values after each cycle of model computation (Hu and others, 2009; George and others, 2012). The fMOR factor assisted in dealing with the difference in time scales between hydrodynamic and morphological developments. It works by multiplying the changes in bed sediments by a constant factor, thereby effectively extending the morphological time step, but significantly reducing computation time. Ranasinghe and others (2011) conducted a sensitivity analysis of fMOR and found that the highest reported fMOR values used in simulations including wave forcing (on highly schematized bathymetries) are limited to about 50. Values of fMOR of 5 and 10 were used to represent morphological change over 5 and 10 years with the assumption that the normal wind, waves, and tidal conditions in a year are the same for the consecutive years.

Model Setup

Model Domains

Four-level nested computational domains were designed and set up (fig. 6). The level-1 ocean-scale domain, which covered part of the North Atlantic Ocean, Gulf of Mexico, and Caribbean Sea, provided water level boundary conditions to the level-2 regional domain. As shown in figure 6*A*, the ocean-scale mesh was refined near the landfall location of Hurricane Sandy. The level-3 basin-wide domain received boundary conditions, that is, current conditions at the north, and water level conditions both at the west and at the east, from the regional domain, and provided water level conditions to the level-4 bay-wide domain. Waves were calculated in all domains. Sediment transport was considered starting from the regional domain. Trachytopes of vegetation and morphological change were applied in level-3 and level-4 domains. Domain properties, such as size and resolution, can be found in table 1. The 10-m resolution was achieved in the bay-wide domain. Due to its size and the small flow time step required, the level-4 bay-wide domain is not suitable for simulation periods of several months or longer. It was used for short-term (for example, 4-day) events only.

Model Parameters

Topography and bathymetry data for Jamaica Bay and saltmarsh wetlands (North American Datum of 1983 [NAD 83], UTM Zone 18, and North American Vertical Datum of 1988 [NAVD 88]) were derived from two sources: (1) National Oceanic and Atmospheric Administration (NOAA) and Federal Emergency Management Agency (FEMA) bathymetry data (interpolated from 30-m to 2-m horizontal resolution) (National Oceanic and Atmospheric Administration, 2010; Federal Emergency Management Agency, 2014); and (2) USGS Coastal National Elevation Database (CoNED) program 2014 topography (1-m resolution, based on lidar data) and bathymetry (10-m resolution) (Danielson and others, 2016). Final topobathy data for Jamaica Bay were interpolated at a cell size of 1 m. Bathymetry data for level-1 and level-2 domains were interpolated from the ADCIRC mesh data (SL16) (Dietrich and others, 2011). The ADCIRC mesh data also provided the distribution of Manning's *n* to determine bottom friction.

Vegetation distribution and plant biophysical properties were incorporated into the sediment transport and wetland morphology model to examine the effect of vegetation on the wetland morphological change under hurricane conditions. The first step in creating the vegetation distribution input grid for Jamaica Bay was to classify each cell as land or water, thereby enabling the isolation of only the land portion for vegetation classification. This land/water classification was accomplished by using unsupervised classification. Classes were interpreted by an image analyst and recoded to land and water categories. Vegetation distributions were classified by using decision tree (DT) classification analyses and rule sets produced by Rulequest See5 in combination with ERDAS IMAGINE 2010. The DT classification analyses use dependent variables (that is, reference or training data) and a suite of predictor variables (that is, independent spatial variables) to develop multivariate classification trees for classifying a target area. Vegetation classification was conducted on several spectral layers and ancillary datasets including the color-infrared (CIR) aerial imagery (June 22, 2013, 1-m resolution), multispectral satellite imagery, and lidar. A training dataset was compiled from multiple sources, including updated National Wetlands Inventory (NWI) data for Jamaica Bay (Bill Jones, USGS, written commun., January 21, 2015); a 2008 saltmarsh distribution across the bay (QuickBird) (Wang and others, 2010); and 2014 field survey on fringe marshes during this study. The final vegetation map (fig. 7) has nine classes: water, mudflat, rocky shore, low marsh, high marsh, formerly connected (*Phragmites*), estuarine shrub/scrub, wetland forested, and upland (table 2).

Table 1. Domain properties of the salt marsh morphology modeling system for Jamaica Bay, New York City.

[s, second; h, hour; km, kilometer; m, meter]

Level	Domain	Size (cells)	Grid spacing	Bay resolution	Flow time step (s)	Wave time step (h)
1	Ocean-scale	253×238	6–40 km	9 km	360	1
2	Regional	411×583	75 m – 2 km	100 m	30	1
3	Basin-wide	156×511	50–175 m	50 m	12	1
4	Bay-wide	686×1,711	10–15 m	10 m	3	1

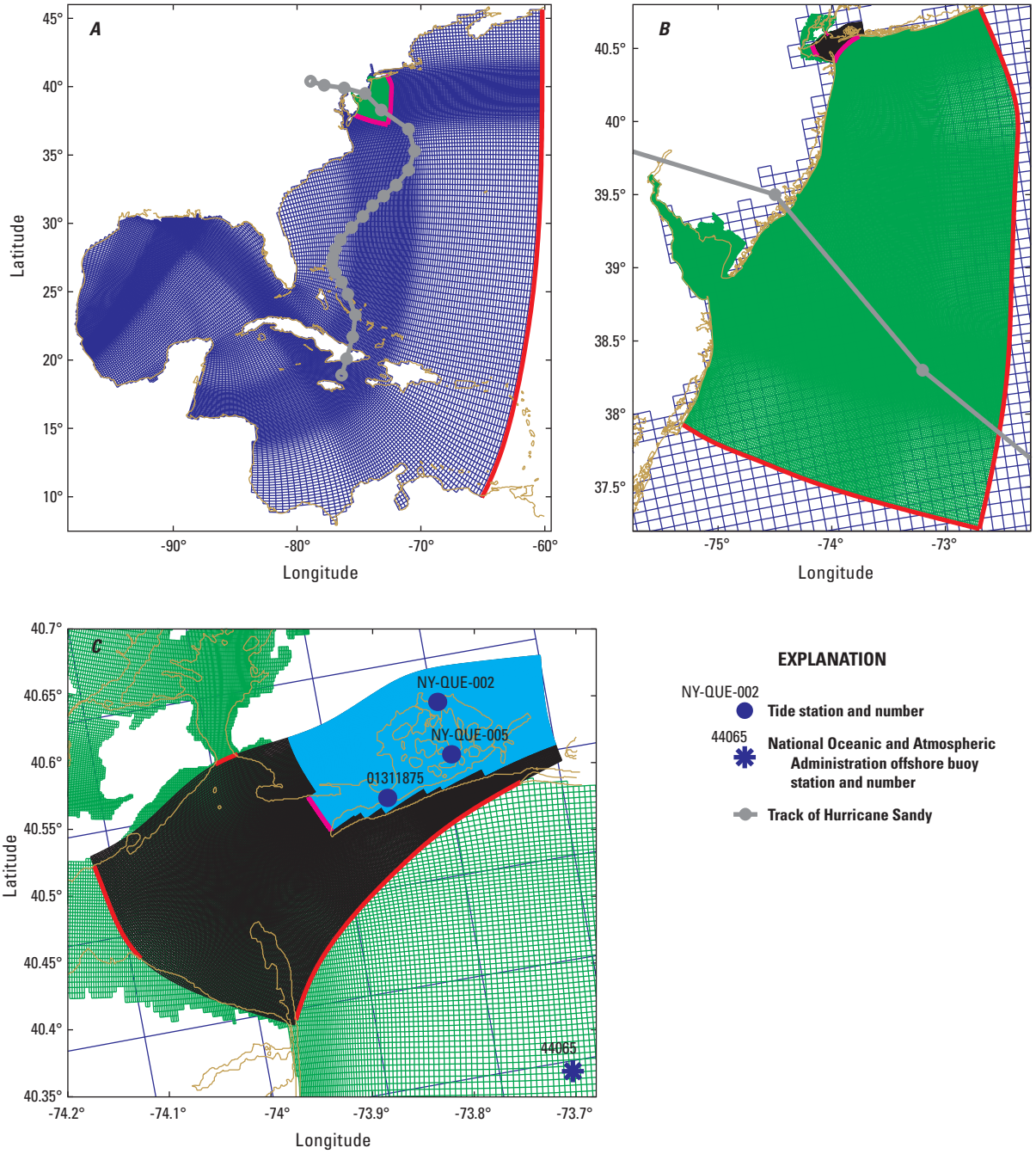

Figure 6. Model domains: *A*, ocean-scale, *B*, regional, *C*, basin-wide and bay-wide, the track of Hurricane Sandy (in *A* and *B*), and locations of tide stations within Jamaica Bay and the National Oceanic and Atmospheric Administration offshore buoy station (in *C*).

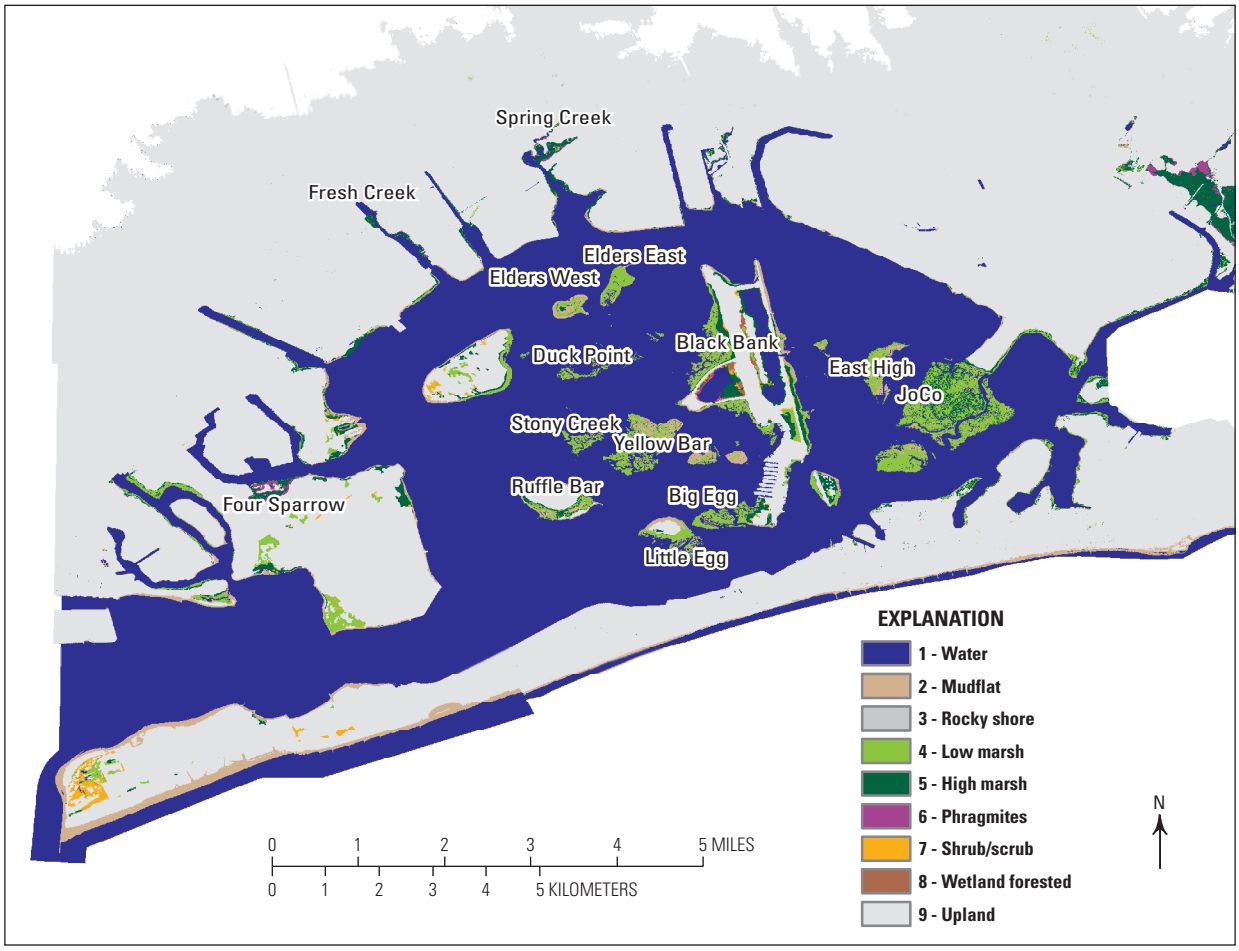

Figure 7. Distribution map of vegetation types across Jamaica Bay, New York City.

Table 2. Vegetation properties used in the salt marsh morphology modeling system for Jamaica Bay, New York City.

[# m^{-2}, number of species per square meter; cm, centimeter; m^{-1},

Type[1]	Common species[2, 3]	Density (# m^{-2})	Height (cm)	Diameter (cm)	Density* diameter (m^{-1})
Low marsh	*Spartina alterniflora*[3]	86	27	0.48	0.41
High marsh	*Spartina patens, Distichlis spicata, Juncus gerardii*[3]	591	32	0.07	0.41
Formerly Connected (Phragmites)	*Phragmites australis*[3]	100	168	0.46	0.46
Estuarine shrub/scrub	*Iva frutescens, Baccharis halimifolia, Morella pensylvanica, Prunus maritima, Rhus* spp.	[4]0.12	[5]175	[5]1.30	0.0016
Wetland forested	*Celtis occidentalis, Prunus serotina, Salix pentandra, Ilex opaca*	[4]0.15	[5]1,200	[5]53.50	0.08

[1]U.S. Fish and Wildlife Service, 2017; New York State Department of Environmental Conservation, 2017.

[2]Nordenson and others, 2015.

[3]Based on measurements by Rebecca Swadek and Christopher Haight, New York City Department of Parks & Recreation, written commun., 2015.

[4]Transactions of the Linnaean Society of New York, 2007.

[5]U.S. Department of Agriculture, Natural Resources Conservation Service, 2017.

Vegetation parameters included (1) species composition, (2) plant height (specifically stem height for marsh species: the point at which the last leaf branches from the plant, the effective height for surge reduction and wave attenuation [Chen and others, 2016; Zhao and Chen, 2016]; total height for wetland shrub, scrub, and trees), (3) diameter (diameters at ¼ stem height for marsh species, at breast height for shrub/scrub and trees), (4) density (the number of stems for marsh species and number of large trunks for shrub/scrub and trees in an area) of the dominant or common species, and (5) percent cover. The data for *Spartina alterniflora* (smooth cordgrass), *S. patens* (saltmeadow cordgrass), and *Phragmites australis* (common reed) were estimated from field measurements in November 2014 in multiple 0.25-m^2 sub-quadrats of 1-m^2 quadrats of salt marshes in Spring Creek and Gerritsen Creek (Rebecca Swadek and Christopher Haight, New York City Department of Parks & Recreation, written commun., March 24, 2015). The biophysical properties for the estuarine shrub/scrub and wetland-forested classes were derived from the literature and are listed in table 2.

Two groups of sediment, mud and sand, were considered in the sediment transport model. Their parameters are listed in table 3. Most of the parameters were set as their default values in Delft3D. The critical bed shear stress for sedimentation was set to be large enough to allow sedimentation all the time. The critical bed shear stress for erosion was calibrated based on vegetation types (table 2). The calibrated values are 0.11, 0.2, 0.4, 0.5, 1.0, 1.5, 1.5, 1.5, and 2.0 Newtons per square meter (N/m^2) for water, mudflat, rocky shore, low marsh, high marsh, formerly connected, estuarine shrub/scrub, wetland forested, and upland, respectively. The initial composition of mud and sand at bed was extracted from the usSEABED data (Williams and others, 2006), along with observations from Renfro and others (2010) and observations from field data collected during this project. Mudflat samples to a depth of 50 cm were collected at 12 sites in Jamaica Bay when marsh cores were collected (see details in the "Model Validation" section). Samples were sectioned into 0–10, 10–20, 20–30, 30–40, and 40–50 cm in order to be analyzed for fractions of mud, which is composed of clay (<4 micrometers [µm]) and silt (40–63 µm), and sand (>63 µm) using the method of Xu and others (2014). Based on sediment samples taken from the Jamaica Bay bottom (Renfro and others, 2010) and mudflat (this study), two representative fractions were determined: a noncohesive sand fraction with d_{50} = 180 µm and a mud fraction.

Table 3. The model parameters used in the salt marsh morphology modeling system for Jamaica Bay, New York City.

Cohesive sediment (mud)		Non-cohesive sediment (sand)	
Reference density for hindered settling	1,600 kg/m^3	Reference density for hindered settling	1,600 kg/m^3
Specific density	2,650 kg/m^3	Specific density	2,650 kg/m^3
Dry bed density	500 kg/m^3	Dry bed density	1,600 kg/m^3
Settling velocity	5×10^{-4} m/s	Median grain diameter	2×10^{-4} m
Initial thickness at bed	Space varying	Initial thickness at bed	Space varying
Critical bed shear stress for sedimentation	1,000 N/m^2		
Critical bed shear stress for erosion	Space varying (calibrated)		
Erosional parameter	6×10^{-6} $kg/m^2/s$		

Initial and Boundary Conditions

Initial conditions for water level, current, and sediment concentration were all set to zero. Initial thickness of sediment at bed was set to 0.4 m. From a tidal constituent database (Mukai and others, 2002), seven dominant constituents (O1, K1, Q1, M2, N2, S2, and K2) were considered to determine tidal levels at the open-sea boundary in the ocean-scale domain. Other boundary conditions including water level, current velocity, and sediment concentration at the smaller domain were interpolated from the larger domain by nesting tools in Delft3D.

Model Calibration

Model calibration efforts were focused on wetland morphological changes. Some sediment parameters, such as critical bed shear stress for erosion, erosional parameter, and settling velocity, were found to be critical for sediment transport and morphological modeling (George and others, 2012; Xu and others, 2015; Liu, 2016) and thus need to be calibrated before they can be used to examine effects of a hurricane on wetland morphological changes.

The National Park Service (NPS) has been studying marsh elevation change and vertical accretion in Jamaica Bay using the rod surface elevation table (RSET) and feldspar marker horizon (MH) techniques (Cahoon and others, 2006). The NPS has collected multiple years of elevation change and vertical accretion data for the marsh surface in Jamaica Bay including a period during Hurricane Sandy. These field observations were used for model calibration and validation (James Lynch, National Park Service, written commun., January 23, 2015). Seven sites with 3 stations at each site (a total of 21 stations) on 5 marsh islands in the bay were established by the NPS since 2002 (fig. 8). At each station, measurements of elevation change and marsh vertical accretion were collected two or three times per year. Normally, vertical accretion data should be used because the morphology model does not consider subsurface processes such as root growth and subsidence due to compaction and organic matter decomposition. Nevertheless, the measurements of elevation change at the sites with both RSET and MH data (except Big Egg Spray) showed similar and consistent results with vertical accretion, suggesting that surface processes such as sediment deposition and erosion mainly determined the elevation dynamics (Cahoon and others, 2006) during the period of measurements

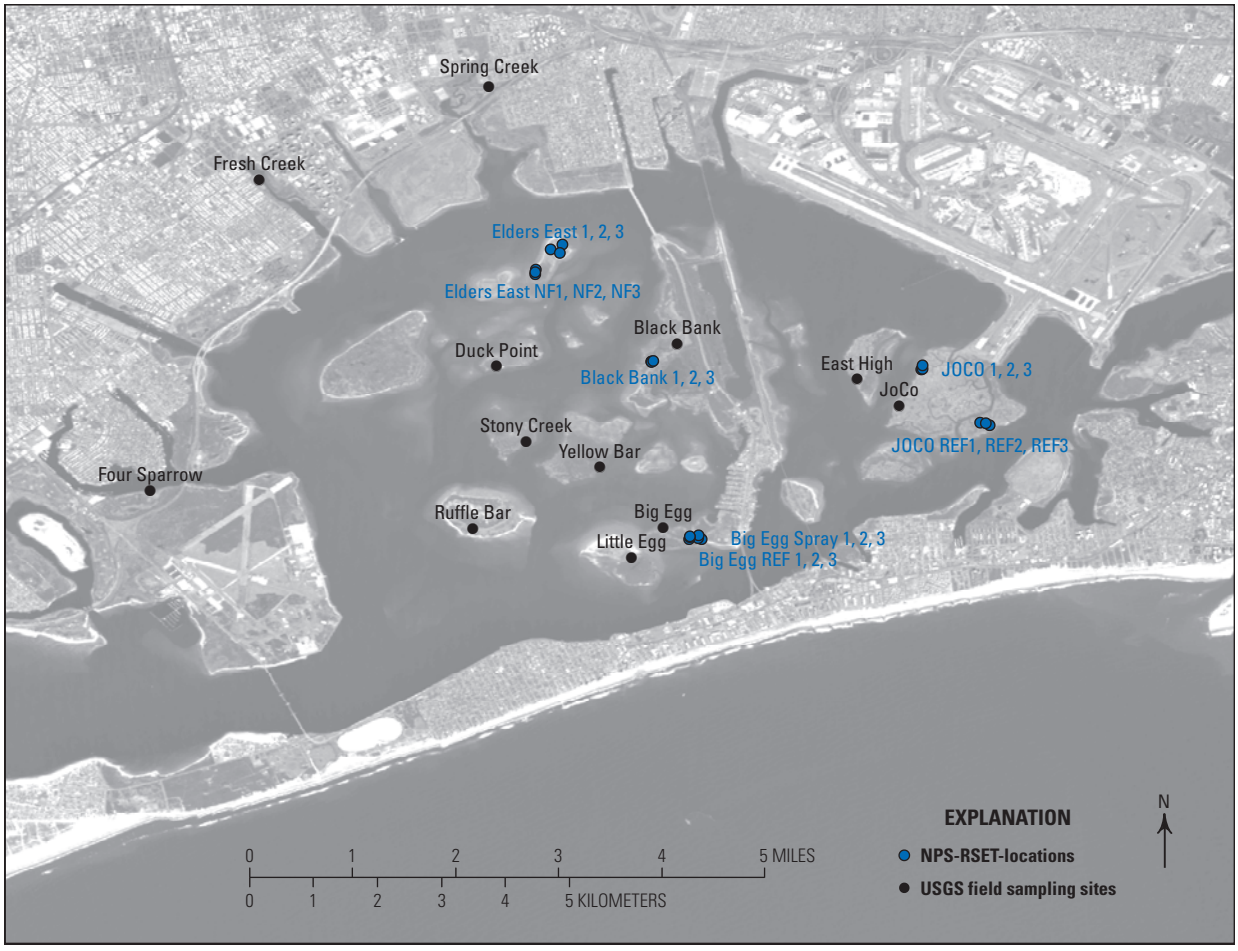

Figure 8. Locations of the rod surface elevation table and marker horizon measurements by National Park Service and field sampling for marsh core collection in Jamaica Bay salt marshes, summer 2014.

at these marshes. Therefore, elevation change data from RSET were also used for model calibration and validation. Measurements of elevation change and vertical accretion over the multiple years since establishment were converted to annual rates for model calibration. Furthermore, the elevation change and vertical accretion during the period October 24 to December 5, 2012 (42 days post-Sandy) were also estimated and used for model validation for Hurricane Sandy effects. The various measurements between elevation change from RSET and vertical accretion from MH during this short period at the same sites were treated as the potential range of the morphological changes due to Hurricane Sandy for model validation.

The calibration was conducted in the level-3 basin-wide domain. The modeling system ran 1 year to get the calculated morphological change rates at these marsh locations for comparison. The results with calibrated parameters are shown in figure 9. The simulated annual morphological changes at these seven marsh sites were close to the field observations (<3 mm for all except the Elders East NF site, a sand beach with very little vegetation) and within the observed ranges (fig. 9).

Model Validation

After the calibration of sediment parameters, the modeling system was further validated by using the in-situ measurements of elevation change and vertical accretion during Hurricane Sandy at the seven marsh sites from the RSET/feldspar data from the NPS and the long-term sediment accretion data collected from multiple salt marshes inside Jamaica Bay during this study. Marsh cores to a depth of 50 cm were collected at 12 sites during August 2014 using 10-cm-diameter, thin-walled, aluminum tubes that were 60 cm in length (fig. 8). The core data were analyzed using the geochronological dating technique following the method of Smith and others (2015). During the lab analysis, partially thawed cores were extruded whole from the aluminum tube, measured, and sliced into 2-cm sections using an industrial band saw. Each section was further divided radially into two subsamples of known volume: 75 percent for radiochemistry and 25 percent for loss-on-ignition and dry bulk density analysis. Long-term vertical accretion rates (VARs) were determined using gamma spectrometry analysis of ^{137}Cs and ^{210}Pb (table 4). The marsh core at Black Bank had a much higher VAR than the upper limit (1.1 cm/yr) determined for Jamaica Bay (Renfro, 2010) due likely to bioturbation (for example, ribbed mussels); thus the VAR at this site was not used in the model validation. The effect of mussel burrows is evidenced by field observation and the reduced soil shear strength in the top 50 cm (<5 kilopascals [kPa]) when compared to that of other marsh sites (15 to 70 kPa) in Jamaica Bay.

Long-Term Simulations

In this study, the morphological acceleration factor, fMOR, was applied to accelerate the morphological evolution to represent long-term wetland morphological changes after Hurricane Sandy. For the non-acceleration case with fMOR=1, the model system runs 1 year after the storm to represent wetland morphological change 1 year after Sandy to see if the storm-induced morphological changes can be recovered after 1 year. For the 5-year and 10-year cases, the model system also runs 1 year, but with fMOR=5 and 10, respectively, to examine how the storm-disturbed wetland morphology will evolve given the similar wave and tide conditions over years excluding the recurrence of a hurricane over the simulation periods (5 and 10 years). The bay-wide domain (10-m spatial

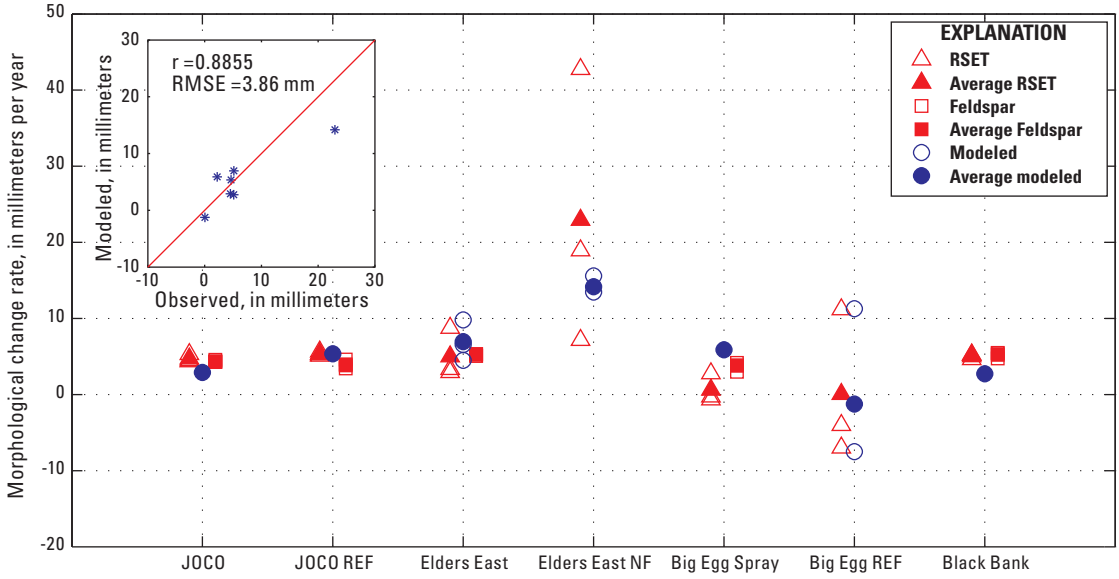

Figure 9. Modeled wetland morphological change rate (short-term, no hurricane) and observations using the rod surface elevation table and marker horizon (feldspar) data at the seven marsh sites in Jamaica Bay, New York City. [RMSE, root mean square error; mm, millimeters]

Table 4. Summary of the long-term vertical accretion rates (VAR) derived from the geochronological dating technique at sampled marsh sites in Jamaica Bay, New York City.

[cm, centimeter; cm/yr, centimeter per year; ND, below detection limits; NA, not applicable]

Core	^{137}Cs 1963 peak depth (cm)	^{137}Cs 1963 VAR (cm/yr)	^{137}Cs 1953 max depth (cm)	^{137}Cs 1953 VAR (cm/yr)	^{210}Pb VAR (cm/yr)
Big Egg	23	0.45	27	0.44	0.36
Duck Point	37	0.73	45	0.74	0.84
Fresh Creek	15	0.29	29	0.48	0.43
Little Egg[1]	ND	NA	ND	NA	0.83
Yellow Bar	17	0.33	19	0.31	0.56
JoCo	25	0.49	31	0.51	0.66
Ruffle Bar	25	0.49	29	0.48	0.5
Stony Creek	21	0.41	25	0.41	0.72
Spring Creek[2]	11	0.22	39	0.64	0.33
East High	23	0.45	25	0.41	0.67
Four Sparrow	23	0.45	25	0.41	0.37

[1]Rapid ^{210}Pb VAR suggests that ^{137}Cs peak is below core maximum depth.

[2]Physical reworking may have resulted in inconsistent 1953 VAR.

resolution) is not suitable for these long-time runs because of the potential model instabilities due to changes in wetting and drying. Thus, model results in the basin-wide domain (50-m spatial resolution) were used for further analyses.

In addition, SLR in 5 and 10 years was considered by adding a time-varying value to the water level boundaries in the basin-wide domain. According to Horton and others (2015b), the local SLR rate in Jamaica Bay was 3.05 mm/yr from 1900 to 2013. In the local domain, the value added to the water level boundaries linearly varies from zero at the beginning to the targeted value in the end of 1 year that the model runs, that is, 15.24 mm for the 5-year case with fMOR=5 and 30.48 mm for the 10-year case with fMOR=10. The SLR was not considered in the 1-year case.

Design of Hypothetical Hurricanes

Hurricane Sandy was a wake-up call for studying hurricane effects on the resilience and stability of coastal wetlands along the Atlantic coast, especially coastal areas of the northeast Atlantic seaboard where a dense human population resides. Given the effect of accelerating SLR and the possibility of more intense hurricanes due to projected climate change (Orton and others, 2012, 2015b, 2016; Horton and others, 2015), it is necessary to predict how future large hurricanes might affect the Jamaica Bay estuary. Orton and others (2016) reviewed historical hurricanes since 1788 that affected New York coastal areas and found that most of these hurricanes had a storm track of 9–30 or 320–359 bearing degrees, maximum wind speed of 28–51 m/s (categories 1–3), and maximum storm surge of 0.9–3.4 m. Therefore, a series of hypothetical hurricanes with varying storm tracks and intensities were designed to investigate the effects of potential future large hurricanes on wetland morphological change in Jamaica Bay. The design was based on Hurricane Irene (2011) and Hurricane Sandy (2012), forming two groups of hypothetical hurricanes: Sandy-like and Irene-like. These two hurricanes are representative of hurricanes, which caused 1.25 m or greater storm surge at New York Harbor since 1788, in terms of storm track and maximum wind speed (Scileppi and Donnelly, 2007; Orton and others, 2016).

The track and landfall location of these hypothetical hurricanes are shown in figure 10. Sandy-like hurricanes, namely SA, SB, and SC, were generated by shifting the Sandy track. SA makes landfall closer to Jamaica Bay than Sandy by 50 percent. SB hits Jamaica Bay directly. SC passes through to the east of Jamaica Bay by a similar distance as SA. In order to test the impact of different wind intensities, the Sandy winds were increased by 10, 20, and 40 percent to generate Sandy-like hurricanes SD, SE, and SF, respectively, with the same pathway as Sandy. The maximum sustained wind speed of Hurricane Sandy near Jamaica Bay was 130 kph (Blake and others, 2013; Sopkin and others, 2014). Based on the Saffir-Simpson hurricane wind scale, the categories of SD, SE, and SF were determined to be 2, 3, and 4, respectively (table 5).

For Irene-like hurricanes, IA and IB were generated by moving the track of Irene 0.5 degree of longitude offshore and landward, respectively (fig. 10). Hurricane Irene made landfall on August 28, 2011, at 13:00 UTC at Coney Island, New York City, with the maximum sustained wind speed of 28 m/s near Jamaica Bay (Orton and others, 2012). IC is a category 2 Irene-like hurricane by increasing the intensity of Irene's winds by 40 percent. The characteristics of these hypothetical hurricanes are summarized in table 5. These storm features were incorporated into the validated Jamaica Bay hurricane-wetland model with new hypothetical wind fields and wind-wave forcing to drive sediment transport, deposition, erosion, and associated morphological changes.

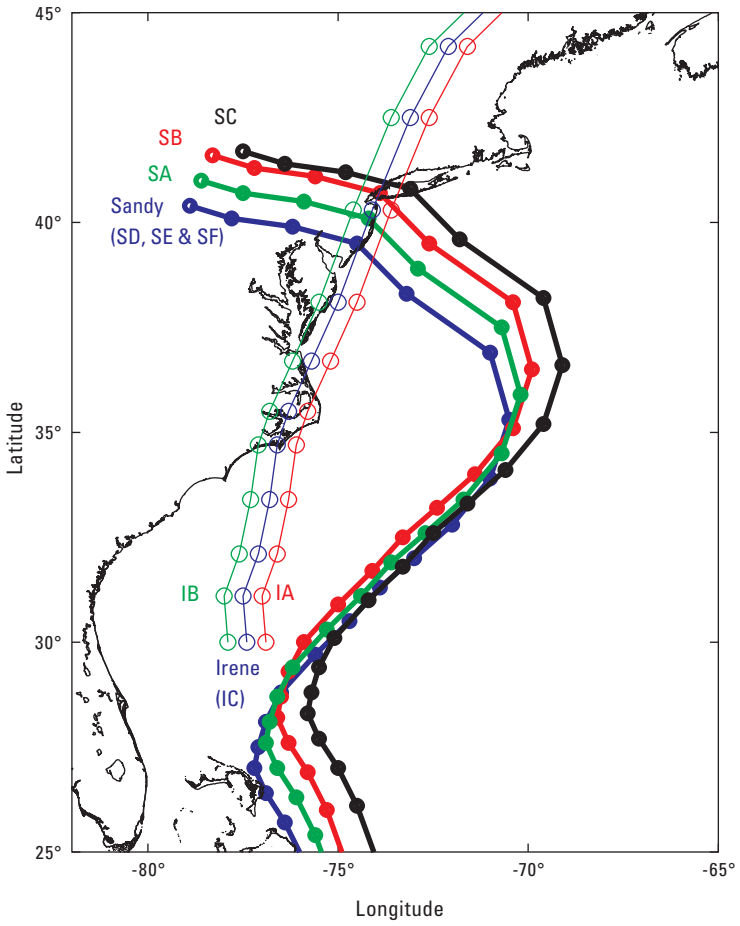

Figure 10. Tracks and landfall locations of hypothetical hurricanes around Jamaica Bay, New York City (see table 5).

Table 5. Summary of the characteristics of the hypothetical hurricanes influencing Jamaica Bay, New York City.

Hypothetical hurricane	Group	Category	Change relative to base hurricane
SA	Sandy-like	2	Make landfall closer to Jamaica Bay by 50 percent
SB	Sandy-like	2	Directly hit Jamaica Bay
SC	Sandy-like	2	Make landfall to the east of Jamaica Bay
SD	Sandy-like	2	Increase intensity by 10 percent
SE	Sandy-like	3	Increase intensity by 20 percent
SF	Sandy-like	4	Increase intensity by 40 percent
IA	Irene-like	1	Move offshore by 0.5 degree of longitude
IB	Irene-like	1	Move landward by 0.5 degree of longitude
IC	Irene-like	2	Increase intensity by 40 percent

Results and Discussion

The results of model validation including salt marsh morphological change, wind speed, wind direction, wave height, wave direction, peak wave period, and water levels are described in the section "Model Validation." The effects of Hurricane Sandy on hydrodynamics, sediment transport, and salt marsh morphology and the effects of hypothetical hurricanes on salt marsh morphology in Jamaica Bay are presented and discussed in the sections "Bay-Wide Sandy-Induced Hydrodynamics and Sediment Transport," "Effects of Hurricane Sandy on Bay-Wide Salt Marsh Morphology," and "Effects of Hypothetical Hurricanes."

Model Validation

Site-Specific Long-Term Morphological Change

The geochronology-based long-term sediment accretion rates at the salt marsh sites in Jamaica Bay ranged from 0.22 to 0.84 cm/yr (table 4). At each site, the three methods (^{137}Cs 1953, ^{137}Cs 1963, and ^{210}Pb) produced various vertical accretion rates, which can be treated as the potential upper and lower limits for annual accretion over a decadal time scale. Big Egg and JoCo are the two sites with accretion estimates from the geochronological approach and RSET/MH. The long-term sediment accretion rates are compatible with RSET/MH-based short-term accretion rates measured since 2002 at the two sites (fig. 8), suggesting that these long-term rates can be used for comparing modeled long-term wetland morphological changes. In relatively healthy marshes such as JoCo and East High in the eastern part of the bay, the long-term accretion rates ranged from 0.45 to 0.67 cm/yr; at marshes in the west, the accretion rates varied from 0.31 to 0.83 cm/yr. In the three fringe marsh sites around the perimeter of the bay, the accretion rates were in the range of 0.22–0.64 cm/yr (table 4). Observed and modeled decadal morphological changes are compared in figure 11. Model results showed some overestimation (<0.4 mm/yr) at Big Egg, Little Egg, and Stony Creek. At the rest of the sites, the modeled rates agreed well with the observed long-term accretion rates, suggesting that the coupled modeling system is capable of capturing long-term (decadal) wetland morphological changes.

The observed and simulated accretion rates are generally consistent with a previous study (Kolker, 2005), in which marsh accretion rates were 0.28, 0.44, and 0.52 cm/yr at JoCo, East High, and Big Egg marshes, respectively. Except

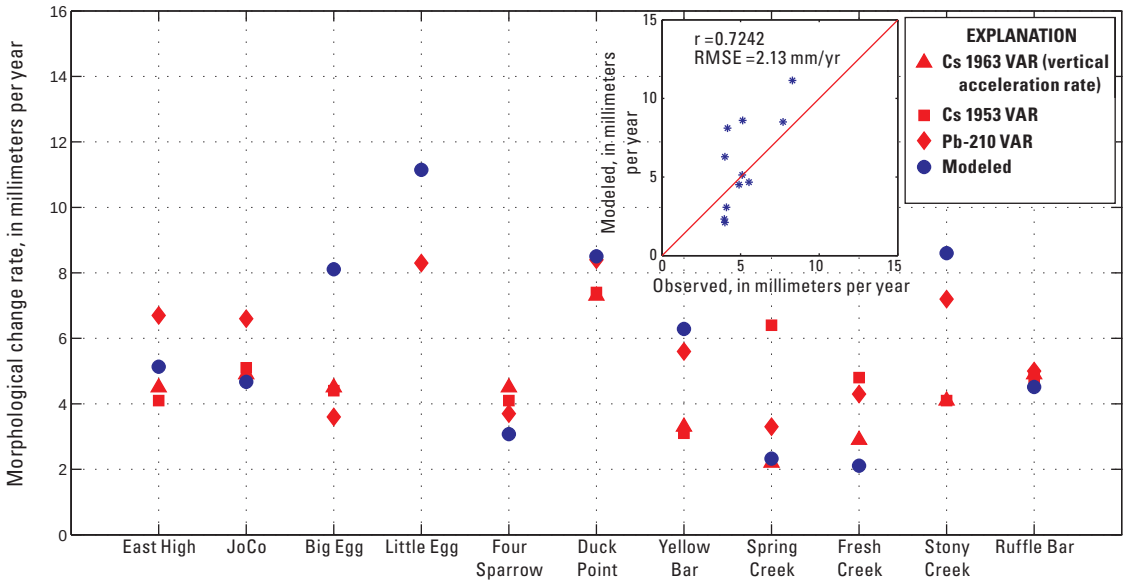

Figure 11. Modeled long-term (decadal) wetland morphological change and observed rates derived from the geochronological dating technique at marsh sites in Jamaica Bay, New York City. [RMSE, root mean square error; mm/yr, millimeters per year; SAR, sediment accumulation rates, mm/yr]

for Fresh Creek and Spring Creek, which are located in the fringe marsh areas of the bay, other sites on interior marsh islands showed higher accretion rates (table 4) than the SLR of 0.3 cm/yr during 1900–2013 (Horton and others, 2015). Marsh accretion rates seem to be generally sufficient to keep pace with RSLR. However, higher-than-SLR vertical accretion rates do not necessarily mean marshes can survive in future environmental change scenarios, including climate change, accelerated SLR, and hurricanes with increased frequency and intensity. Horton and others (2015b) projected that SLR during the next 50–100 years in the New York area will likely be >10 mm/yr and accelerating over the years. These long-term accretion rates (<10 mm/yr) indicate that salt marshes in Jamaica Bay will most likely not be able to keep pace with SLR, thereby converting to nonvegetated mudflat or open water. Furthermore, it was realized that horizontal dynamics and related sediment fluxes are the key factors determining the survival of salt marshes (Fagherazzi and others, 2013a). The vertical accretion rates of these surviving marsh sites could not be applied to the already-lost marshes because of the lack of data on wave-driven erosion because marshes are horizontally disappearing due to increased ponding within marsh interiors, slumping along marsh edges, and widening of tidal creeks (Hartig and others, 2002).

Wind, Waves, and Storm Surge During Hurricane Sandy

The nested, coupled modeling system was applied to Hurricane Sandy to test the model performance under hurricane conditions. The model ran 30 days before the event to attain reasonable initial conditions. Then it ran 4 days from October 28 to 31, 2012, during which Hurricane Sandy made landfall and passed through the northeast Atlantic coast. During this period, waves were coupled with currents in model simulations. The comparisons of wind and wave parameters, water levels, and morphological change with measurements during Hurricane Sandy are shown below to demonstrate the acceptable model performance.

Simulated and observed wind speeds and wind directions at the NOAA offshore buoy 44065 (see fig. 6 for its location) in the regional domain are shown in figure 12. In addition, scatterplots with correlation coefficient (r) and root mean square error (RMSE) for each wind parameter are provided. Good agreement between the model and observations demonstrated that the asymmetric wind model (Hu and others, 2012) is able to capture wind fields caused by large hurricanes, although it tends to overestimate peak and underestimate non-peak wind speeds with an overall RMSE of <4 m/s (fig. 12). The wind model successfully captured the turning of wind direction when Hurricane Sandy made landfall (fig. 12).

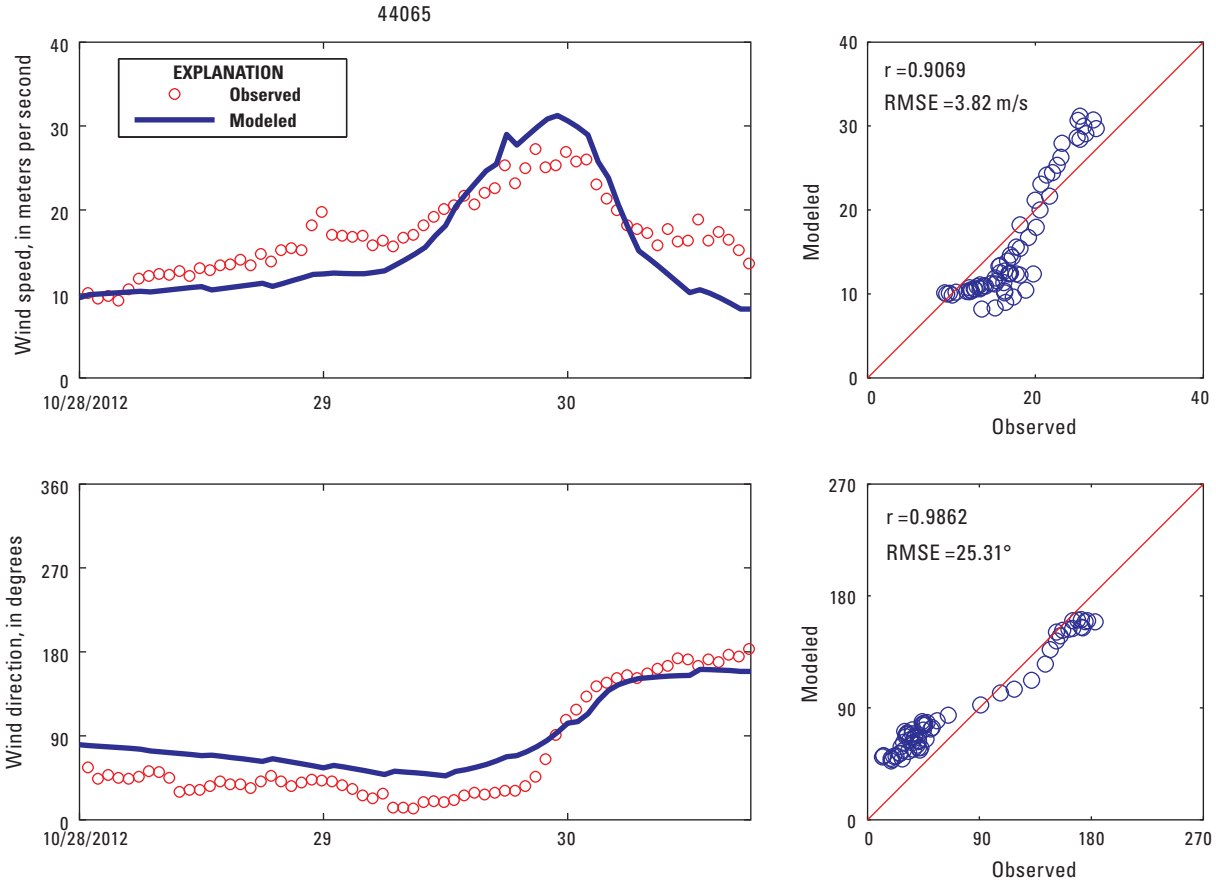

Figure 12. Simulated and observed wind speeds and wind directions during Hurricane Sandy at National Oceanic and Atmospheric Administration National Data Buoy Center buoy station 44065. [m/s, meters per second; RMSE, root mean square error]

Figure 13 shows simulated and observed significant wave heights, wave directions, and peak wave periods at the NOAA offshore buoy 44065 in the regional domain. The model tracked the observed significant wave height from growth through the peak and then decay (fig. 13) despite the underestimation of the maximum wave height (about 9.9 m at 00:50 UTC on October 30, 2012) (Sopkin and others, 2014). The modeled wave direction and peak wave period generally followed the measurement trends (fig. 13). There was a sharp change in wave direction right before Hurricane Sandy's landfall from almost south to east, then gradually back to southwest toward the Jamaica Bay area (fig. 13). The observed and modeled peak wave periods reached 15 seconds during Hurricane Sandy at this station, which could determine the wave-current bed stress (Orton and others, 2012). The values of *r* and RMSE percentage were 0.97 and 12 percent, 0.61 and 15 percent, and 0.55 and 17 percent for significant wave height, wave direction, and peak wave period, respectively, demonstrating that the model is capable of capturing hurricane-induced wave transformation processes near Jamaica Bay. It should be noted that measurements of wave parameters from only one offshore buoy were used because there were no data available from sites within the bay.

The model reproduced the pre-Sandy tides, Sandy-induced storm tide, and post-Sandy tides well (fig. 14). The good agreement between the model and observations at the three interior stations indicated that the modeling system is capable of reproducing the process of storm surge generated by Hurricane Sandy in Jamaica Bay. Observed and modeled water levels showed more than 3 m (NAVD 88) of water level increase induced by Hurricane Sandy in Jamaica Bay.

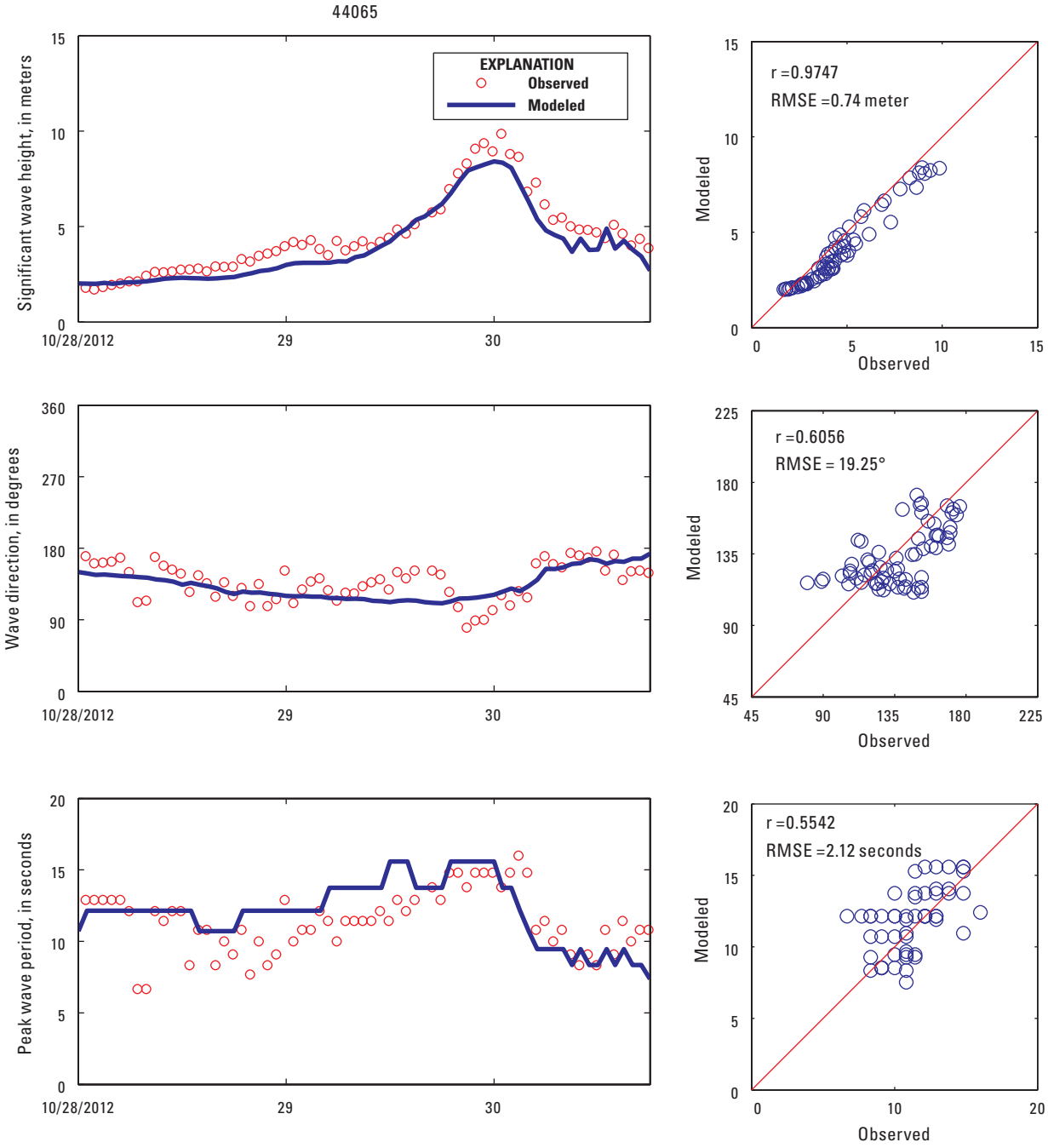

Figure 13. Simulated and observed significant wave heights, wave directions, and peak wave periods during Hurricane Sandy at National Oceanic and Atmospheric Administration National Data Buoy Center buoy station 44065. [RMSE, root mean square error]

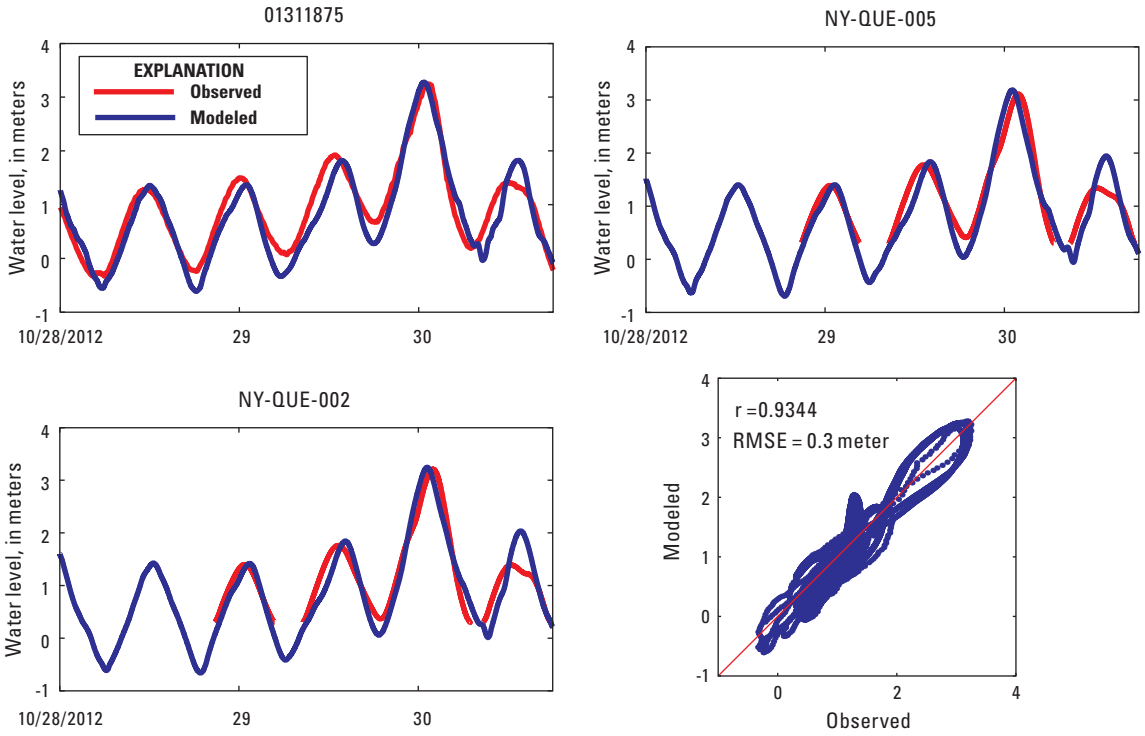

Figure 14. Modeled and observed water levels during Hurricane Sandy at three tide stations in Jamaica Bay, New York City. [RMSE, root mean square error]

Site-Specific Sandy-Induced Morphological Change

The Sandy-induced morphological change was validated by the RSET and MH feldspar measurements before and after the event. The comparisons between the modeled and RSET and MH measured morphological change induced by Hurricane Sandy at seven marsh sites inside Jamaica Bay are shown in figure 15. For each marsh site, measurements were made at three nearby stations. Except for the missing feldspar data at Elders East NF and Big Egg Spray, there are six elevation change datasets, three by RSET and three by feldspar MH (fig. 8). Two averaged values for different methods at each station were included in figure 15 as well. At JoCo, the morphological change was small (less than 5 mm). The modeled results showed mild deposition, which is consistent with measurements. At JoCo REF, deposition and erosion were measured. The modeled results were within the range of observations. The modeled results showed erosion on average at Elders East and Black Bank (fig. 9). At the Elders East NF site, the large erosion (>40 mm) was measured by RSET at two of the three stations. The model results also indicated erosion, but with a reduced magnitude (<30 mm). One possible reason is the lack of vegetation during the field measurement period, whereas the site was covered with low marsh as a result of marsh restoration in the vegetation map used by the model. This also indicates indirectly the importance of vegetation in reducing marsh erosion. At the two sites on Big Egg (Big Egg Spray and Big Egg REF), the model results were generally consistent with the measurements, although the modeled range of morphological change tended to be larger than the measured range.

Bay-Wide Sandy-Induced Hydrodynamics and Sediment Transport

Waves

The distributions of simulated maximum significant wave height, peak wave period, and maximum suspended mud and sand concentrations in Jamaica Bay during Hurricane Sandy are shown in figure 16. At the bay entrance (Rockaway Inlet), the significant wave height and peak period were over 2 m and 10 seconds, respectively. Model results showed that Hurricane Sandy generated large wave energy from offshore passing through the inlet into Jamaica Bay. The simulated Sandy-induced wave height across the bay is consistent with the study (Smith and Anderson, 2014) of vegetation effects on wave reduction under severe wind (26 m/s) and water level (2.9 m) conditions. This study and Smith and Anderson (2014) showed that storm-induced waves with height > 1.2 m grow from Rockaway Inlet, Island Channel and reach the northern shoreline of the bay. As a consequence of Hurricane Sandy, significant wave heights within the bay were dramatically increased. During the hurricane, significant wave heights in areas adjacent to marsh islands could reach >1.2 m, becoming a large force that suspended bottom sediment or caused marsh erosion near the bay's open water boundary and tidal creeks. Modeled maximum suspended sand concentrations in most of the western part of the bay, including marsh areas, tended to be larger than 0.2 kilogram per cubic meter (kg/m^3), whereas maximum suspended mud concentrations greater than 0.2 kg/m^3 tended to be found at the entrance and the eastern part of the bay (fig. 16*C*, *D*), suggesting that sandy materials tend to

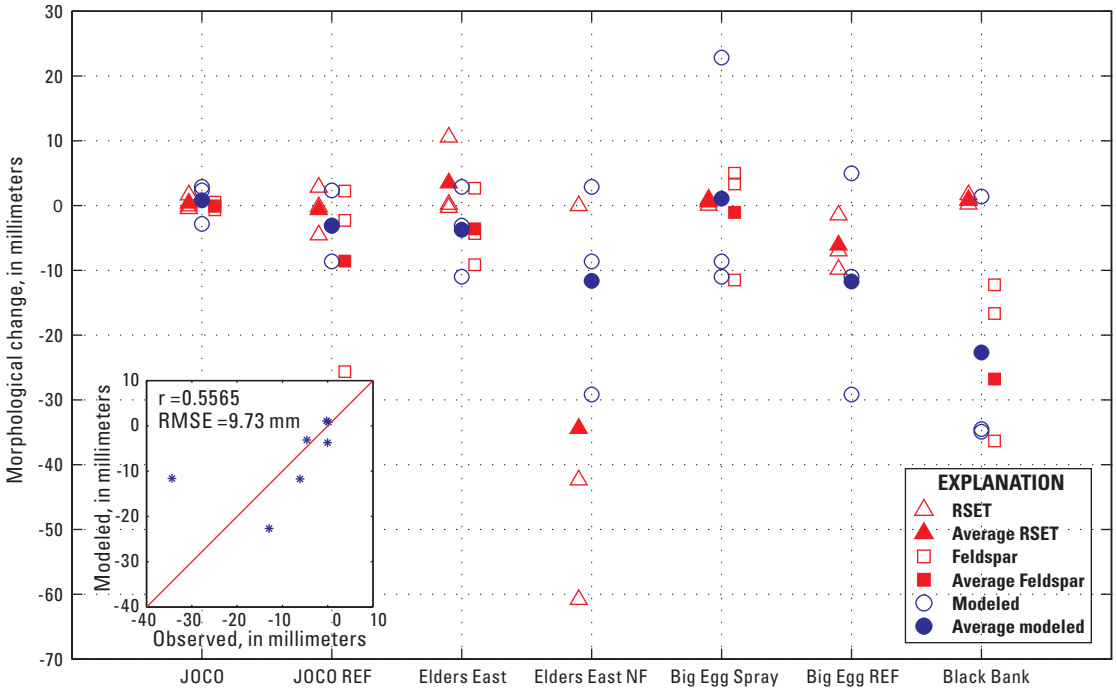

Figure 15. Modeled Hurricane Sandy-induced salt marsh morphological change and observations derived from the rod surface elevation table and marker horizon (feldspar) data at marsh sites in Jamaica Bay, New York City. [RMSE, root mean square error]

dominate morphological change in the west portion of the bay, whereas muddy materials determine the changes in the east portion of the bay.

Because of the nearly enclosed shape of the bay, most waves inside were locally generated, and the wind fetch played a very important role. Hurricane Sandy passed to the south of the bay, which caused easterly and southeasterly winds over the entire bay. Wave heights in the west and north parts of the bay were relatively large due to the relatively long fetches. Wave heights at the eastern part were small, especially at the JoCo marsh, because of short fetches and vegetation. The distribution of maximum peak wave period showed that long waves with large wave period (>8 seconds) were propagated into the western part of the bay from the entrance. The locally generated wind waves cannot have large periods, lasting only about 3 seconds at the eastern part of the bay (fig. 16*B*).

Storm Surge, Current Velocity, and Bed Shear Stress

The Sandy-induced maximum surge, current velocity, bed shear stress, and total sediment transport are shown in figure 17. Due to the easterly winds blowing over the entire Jamaica Bay, the maximum surge (relative to NAVD 88) reached 3.5 m at the northwest corner of the bay, and gradually decreased to 3 m in the eastern part of the bay (fig. 17*A*). The difference in the Sandy-induced maximum surge is less than 1 m across the entire bay. The maximum velocities in channels and shallow bay areas were larger than those on marsh islands. The maximum velocities reached 2 m/s in the channels in the north and the south regions of the bay. On the marsh islands inside the bay, velocities were normally less than 0.5 m/s (fig. 17*B*). The simulated Sandy-induced maximum bed shear stresses showed a complex and heterogeneous spatial pattern across the entire bay. At Rockaway Inlet and in the areas near the inlet, the maximum bed shear stress tended to be larger than 10 N/m^2 whereas the channels around and inside the bay as well as the deep-water areas such as the Grass Bay tended to have smaller bed shear stresses (<1 N/m^2) (fig. 17*C*). In contrast, the simulated maximum bed shear stress in the range of 1–10 N/m^2 tended to intersperse at a local scale in the marsh areas inside the bay especially in marsh areas in the eastern part of the bay (fig. 17*C*). Most of the marsh areas tended to have Sandy-induced maximum bed shear stress larger than 5 N/m^2. In contrast, the shear stress exerted by current and wave velocities within the bay during nonhurricane conditions is seldom greater than 4.8 N/m^2 (New York City Department of Environmental Protection, 2007).

Sediment Transport and Budget

The distribution of maximum total sediment transport rates due to Hurricane Sandy is also shown in figure 17*D*. Considering high current velocities and low critical sediment erosion shear stresses in the channels, sediment transport rates were orders of magnitude higher in the channels than over marsh areas. It appears that large sediment transport was associated with large significant wave height (fig. 16*A*) and maximum current velocity (fig. 17*B*). The hurricane-driven (combined tidal and wind-driven) current velocities with local winds mostly out of south, and along the long axis of the bay and oriented with the two channels (North and Beach) between the western and eastern bay, were sufficient to

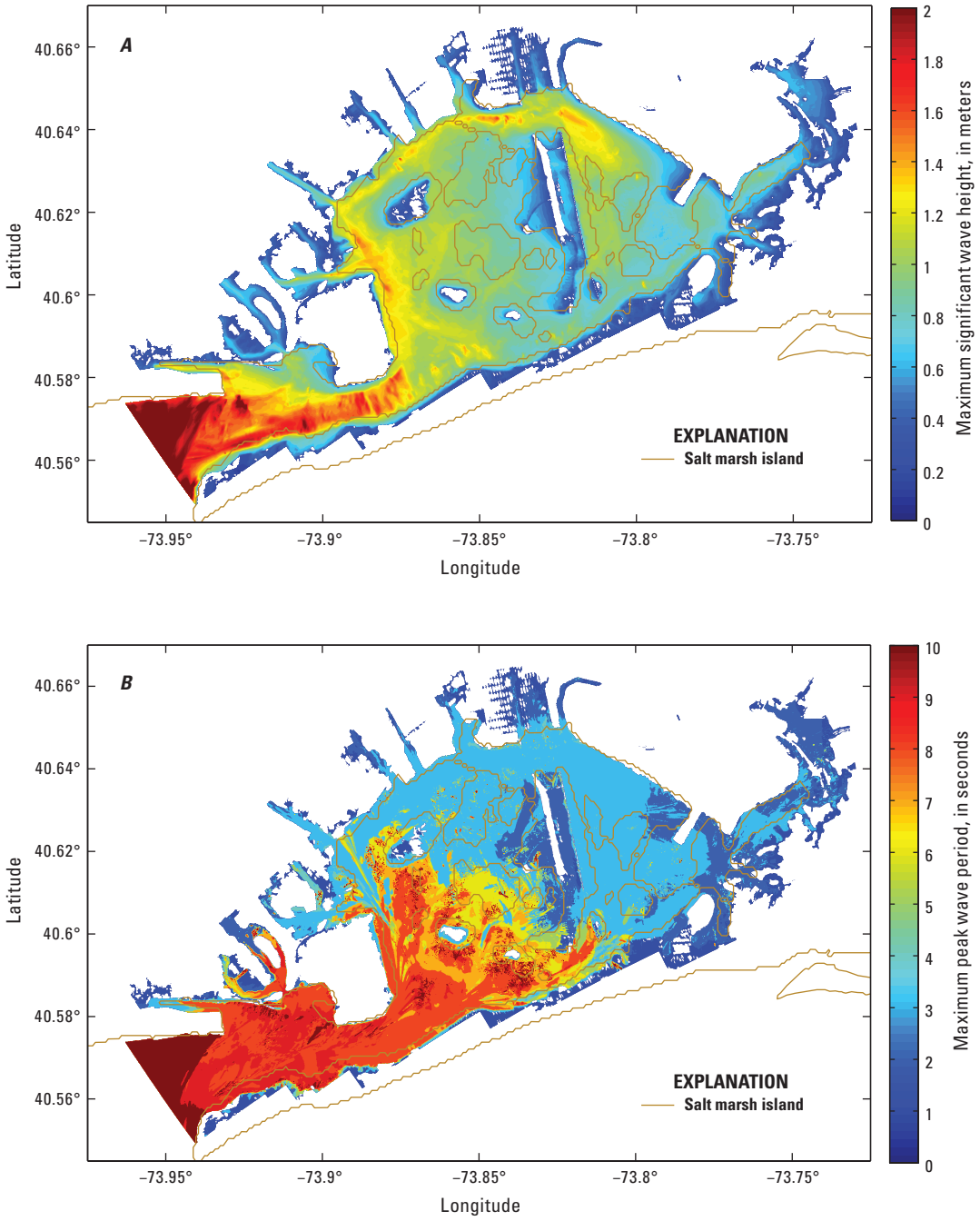

Figure 16. Modeled Hurricane Sandy-induced *A*, maximum significant wave height; *B*, maximum peak wave period; *C*, maximum suspended mud; and *D*, maximum suspended sand concentrations in Jamaica Bay, New York City.

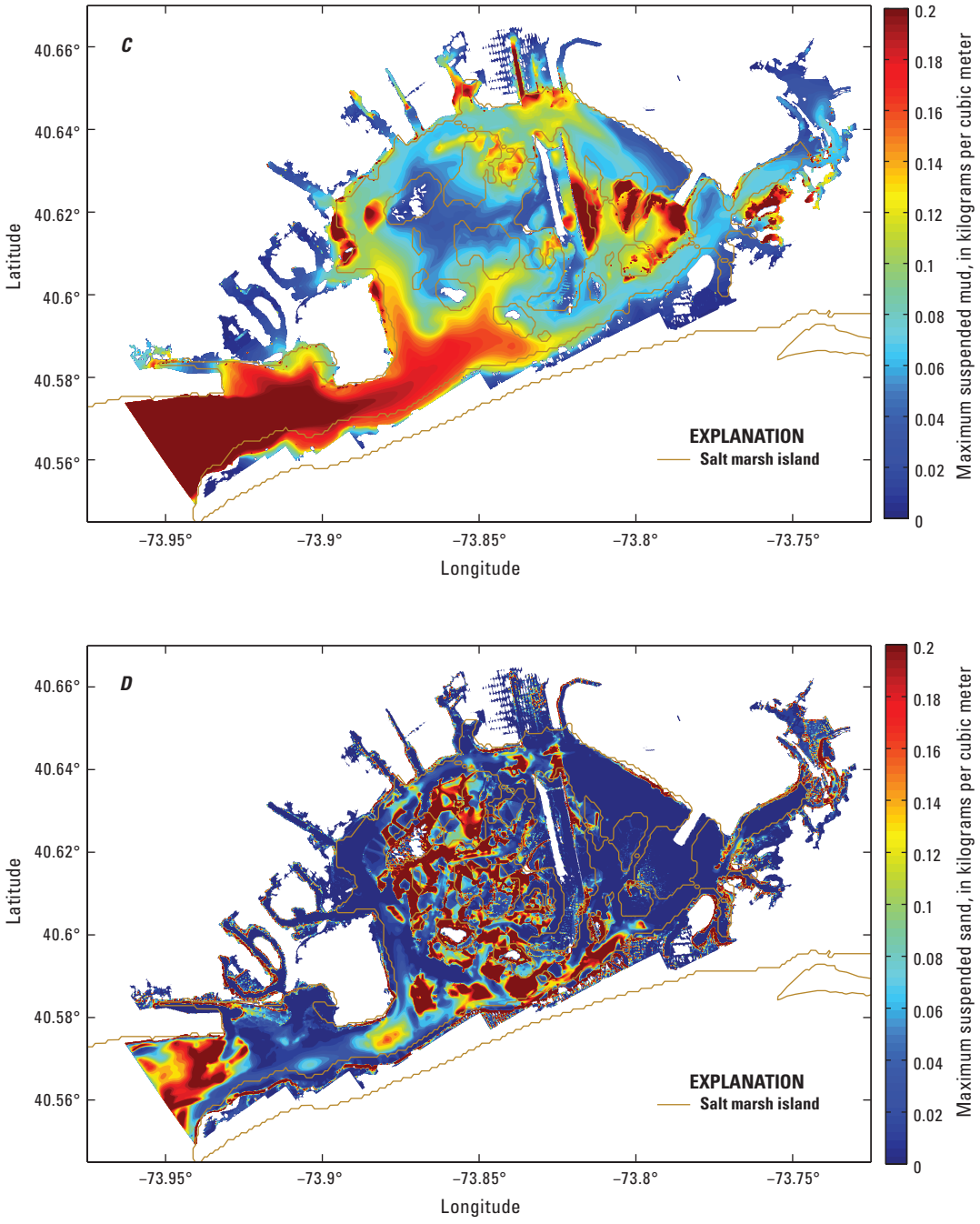

Figure 16. Modeled Hurricane Sandy-induced *A*, maximum significant wave height; *B*, maximum peak wave period; *C*, maximum suspended mud; and *D*, maximum suspended sand concentrations in Jamaica Bay, New York City.—Continued

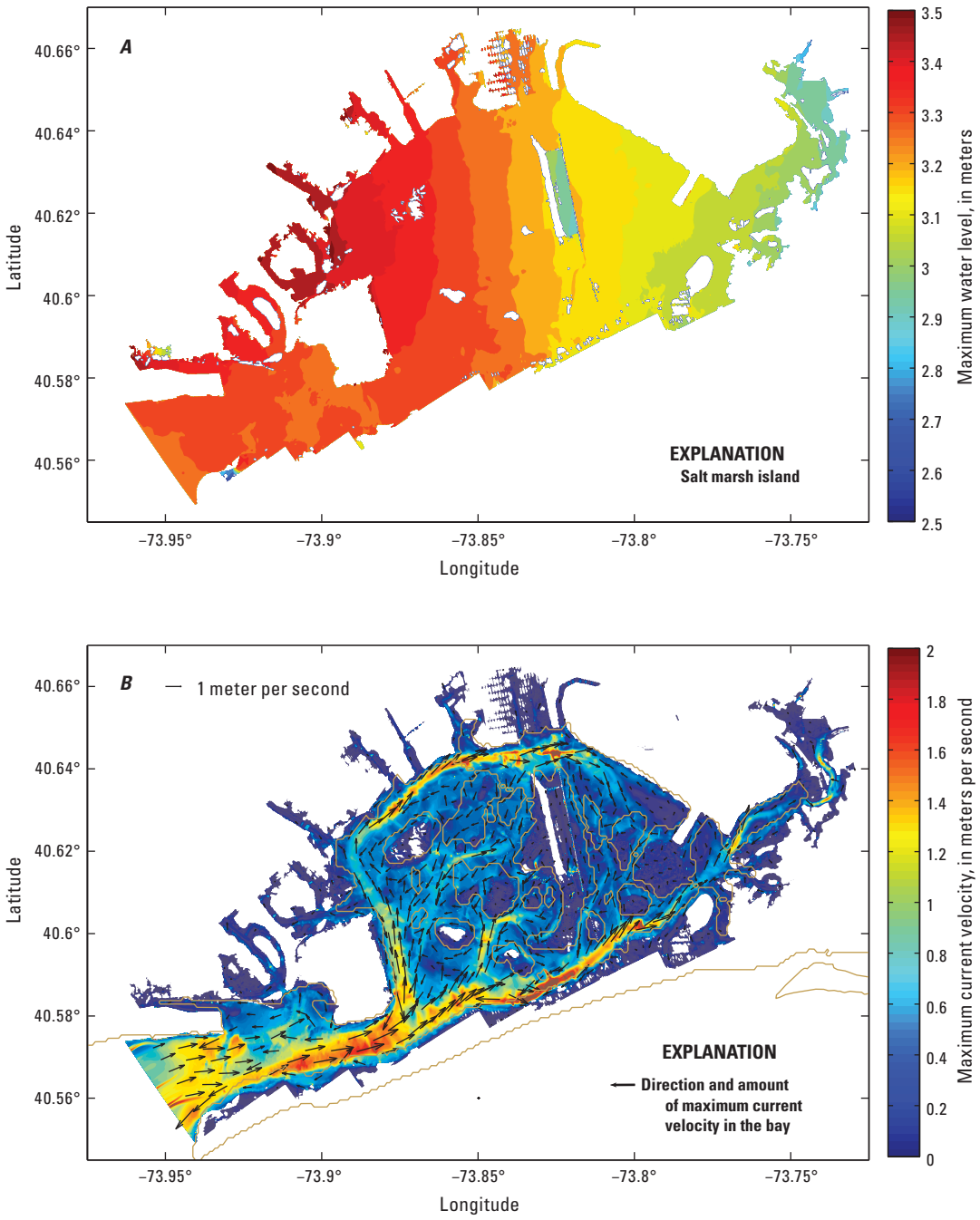

Figure 17. Hurricane Sandy-induced *A*, maximum water level; *B*, maximum current velocity; *C*, maximum bed shear stress; and *D*, maximum total sediment transport (suspended + bed) rates (color bar is log-scale) in Jamaica Bay, New York City. Vectors are plotted with a linear scale.

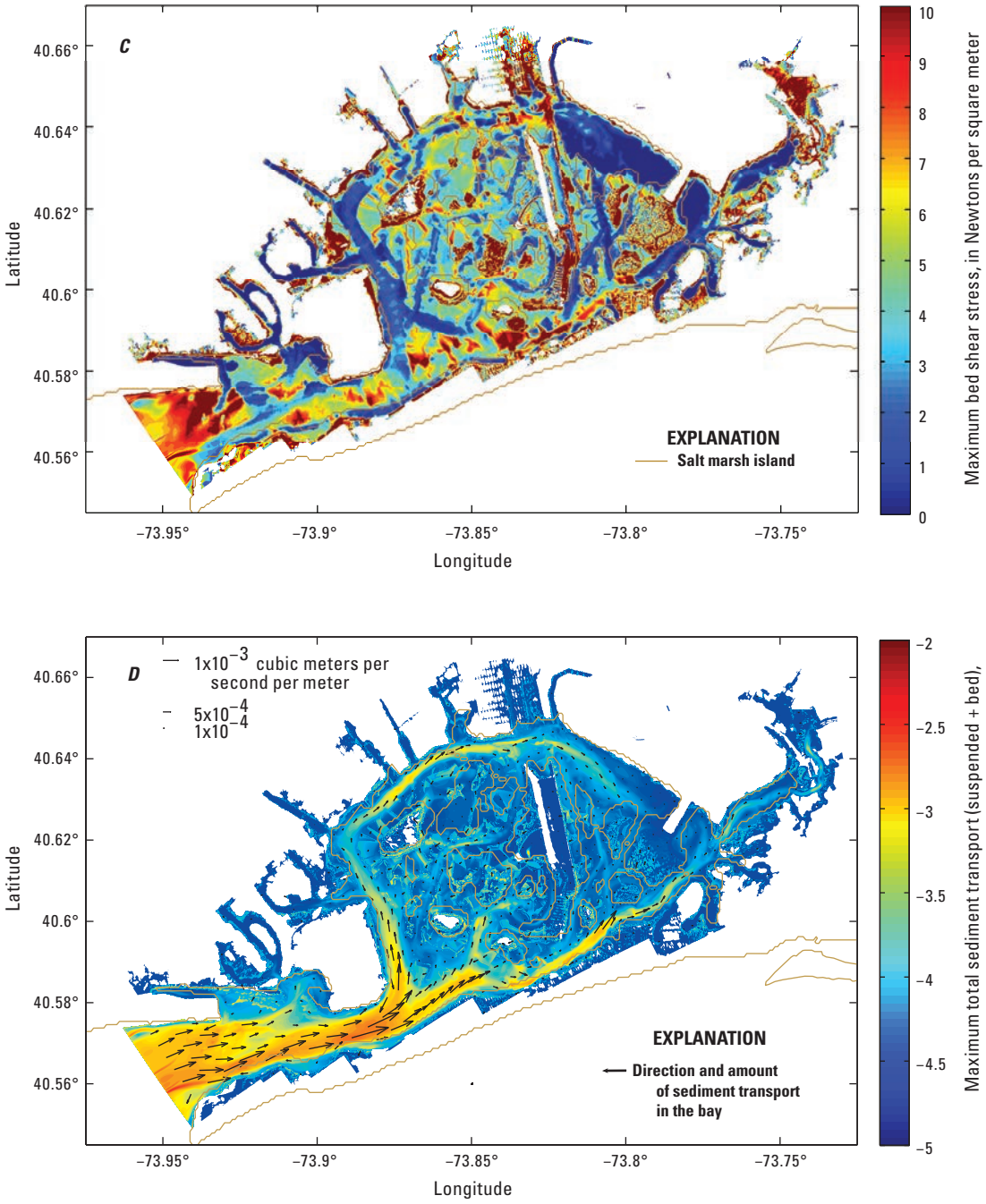

Figure 17. Hurricane Sandy-induced *A*, maximum water level; *B*, maximum current velocity; *C*, maximum bed shear stress; and *D*, maximum total sediment transport (suspended + bed) rates (color bar is log-scale) in Jamaica Bay, New York City. Vectors are plotted with a linear scale.—Continued

redistribute suspended sediments (fig. 16*C*, *D*), allowing them to be deposited in the deeper waters of the bay and onto marsh surface by way of the deep channels around the bay (fig. 2). Although there were no immediate measurements of sediment deposition and erosion post-Sandy, field measurements of thorium-234 in excess (^{234}Thxs) inventories in sub-tidal sediments in November 2005, corresponding to the period right after a winter storm, showed that additional sediments were deposited near western marshes, and also in Grassy Bay (Renfro, 2010), suggesting the capability of storms to transport sediments to the eastern part of the bay by way of channels, sub-tidal bays, and tidal creeks.

The total Hurricane Sandy-generated sediment input (Oct. 27–31, 2012) into Jamaica Bay through Rockaway Inlet was estimated from the coupled hurricane-wetland morphology model to be 9,354 metric tons (*t*) (mud = 4,958 *t*, sand = 4,396 *t*), which represents only about 1 percent of the total amount of reworked sediment (both sediment deposits and erosion) within the bay during Hurricane Sandy. Most of the sediment deposition and erosion came from storm-induced resuspension of bay bottom and eroded marsh soils. Hurricane Sandy resulted in approximately 4,676 *t* of mud and 385 *t* of sand in net suspension in Jamaica Bay and associated inundated marsh areas.

Renfro (2010) used a mass balance of thorium-234 (^{234}Th) in the bay to estimate an annual input of sediment from the New York Bight by way of Rockaway Inlet to be 43,000 to 358,000 MT. Based on this estimate of annual sediment input into the bay, Hurricane Sandy could bring 2.6 to 21.8 percent of the annual total mineral sediment into Jamaica Bay. Considering the fact that the ^{234}Th may overestimate sediment deposition over a full year because ^{234}Th represents short-term patterns (Renfro, 2010), the contribution of Hurricane Sandy to sediment importation from the ocean might be higher than this estimated range.

Effects of Hurricane Sandy on Bay-Wide Salt Marsh Morphology

Short-Term Effects

The immediate morphological change in Jamaica Bay caused by Hurricane Sandy in 4 days (October 28–31, 2012) is shown in figure 18. Hurricane Sandy caused erosion and accretion in Jamaica Bay. For the entire bay, the change was more dynamic in the western part (for example, Yellow Bar) than in the eastern part (e.g., JoCo) of the bay, which is consistent with the distributions of current velocity and sediment transport (fig. 17*B*, *D*). Numerous pairs of erosion and accretion patches suggest that these morphological changes were locally generated as a result of the complex bathymetry in the bay. In some specific wetland areas such as JoCo and Yellow Bar (fig. 18), channels, creeks, and mudflats appear to be eroded. For example, the main channel/creek that divided the JoCo marsh showed obvious erosion while the vegetated area showed erosion and accretion.

Simulation results indicated that larger deposition and erosion (> ±0.15 m) caused by Hurricane Sandy occurred in channels (for example, North Channel and Beach Channel, fig. 2) rather than the tidal creeks and marsh surface and occurred in the western area rather than in the eastern area of the bay. Increased bed shear stress over time, which suspended both muddy and sandy sediments, tended to be the major driver of the sediment deposition and erosion across the bay. Near or in the marsh areas, the bed shear stress was significantly reduced compared to nonvegetated areas, resulting in lower rates of deposition and erosion. A coarsening of the post-Sandy sediment with an increased bed shear stress was found to be the mechanism for morphological change from

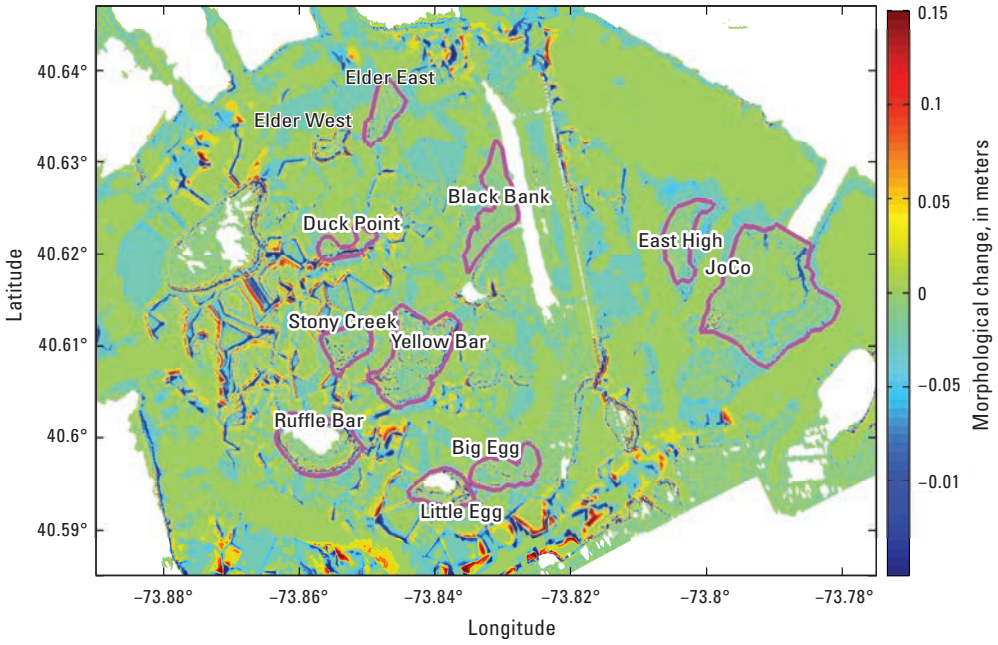

Figure 18. Modeled spatial patterns of morphological change caused by Hurricane Sandy in Jamaica Bay, New York City.

Hurricane Sandy in a back-barrier estuary along the New Jersey coast (Miselis and others, 2015). This study indicated that such a mechanism could also be responsible for the morphological change in the western part of Jamaica Bay, but not for the eastern part of the bay.

The combined wind waves and tidal currents are the processes responsible for sediment resuspension and transport in areas near salt marshes as a result of the increased bed shear stress during the hurricane (fig. 17*C*). High suspended sediment concentration (SSC) during Hurricane Sandy in the western part of the bay is evident (fig. 16*C*, *D*) and is closely related with the storm-induced significant wave height and wave period (fig. 16*A*, *B*). During the hurricane, the wind and wave setup increased the maximum water level through water discharge during storm surge flooding channels. Therefore, during the hurricane, water discharge and sediment concentrations of the entering water increased, resulting in increased total volume of sediment imported into the marsh and the adjacent bay areas. This study is consistent with previous studies that showed that deposition rates could be higher and extend further into marshes during storm tides (Cahoon, 2006; Turner and others, 2006; Fagherazzi and others, 2013b). After the hurricane made landfall, the surge receded (ebb), and the SSC was determined by the processes mobilizing sediment within the salt marsh areas and tidal currents rather than by wind waves. In contrast, sediment was eroded and resuspended from channel bottoms and banks and from mudflats without the vegetation that protects the substrate as is demonstrated by high ebb velocity and bottom stresses (Fagherazzi and others, 2013b).

Figure 19 shows the deposition and erosion patterns caused by Hurricane Sandy in Jamaica Bay. The deposition and erosion were defined as morphological change larger than 5 mm. Areas with change less than 5 mm were shown in green. It can be seen that Hurricane Sandy caused extremely complex patterns of deposition and erosion in Jamaica Bay. Erosion and deposition appeared across the entire bay, either in channels or creeks or on marshes. As discussed earlier, erosion appeared in the main channel of the JoCo marsh island, while in other places, both erosion and deposition were triggered. In order to quantify the effects of Hurricane Sandy on wetlands in Jamaica Bay, 10 marsh islands (figs. 18 and 19) were selected for further analyses.

During Hurricane Sandy, maximum significant wave heights (>1.2 m) and peak wave periods (>6 seconds) were in Rockaway Inlet and in channels around the bay, especially the North Channel, and reached into Grassy Bay located in the eastern area of Jamaica Bay (fig. 16*A*, *B*). These wave factors appeared to be responsible for the larger deposition and erosion in the western part of the bay (fig. 18). As indicated by the studies of hurricanes across a large spatial scale in the northern Gulf of Mexico (Liu and others, 2015; Xu and others,

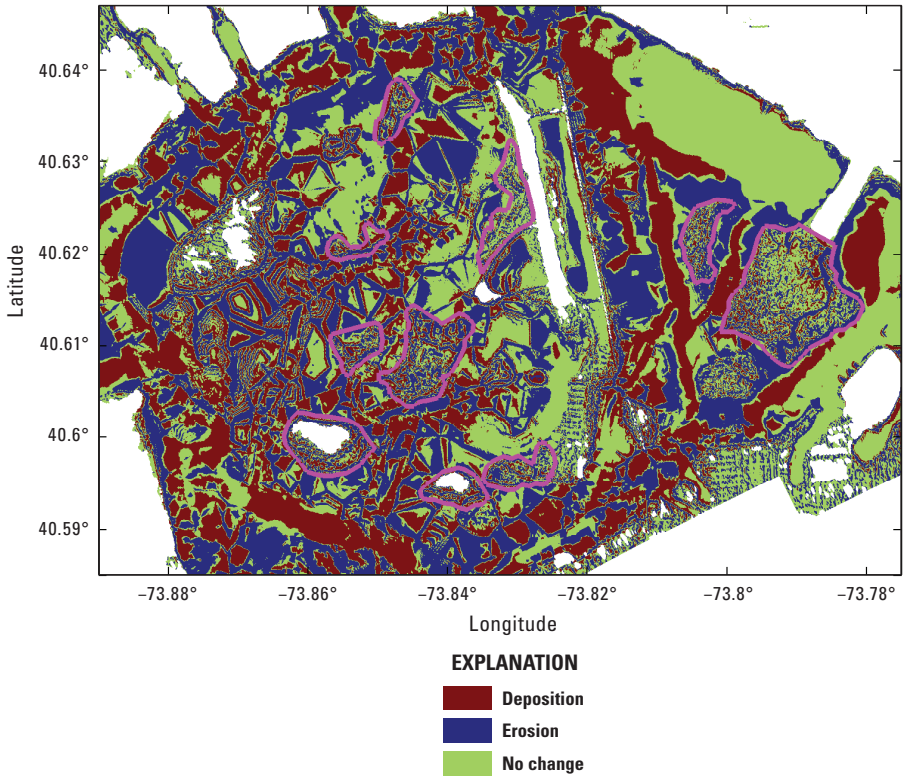

Figure 19. Modeled spatial patterns of sediment deposition and erosion due to Hurricane Sandy in Jamaica Bay, New York City.

2015; Liu, 2016), hurricane-induced waves are the driving forces for sediment resuspension (Xu and others, 2015). The evidence of this is the larger SSC found in the southwestern area of the bay than in the eastern area of the bay (fig. 16*C*, *D*). Wave energy dissipated quickly when reaching the shallow areas of the bay and in the inundated wetland areas where the wave height and current velocity are significantly reduced (figs. 16*A*, 17*C*), causing complex patterns in wave-induced bed shear stress (fig. 17*C*). Large wave-current combined shear stresses were found in the shallow bay, creek banks, tidal flat, and marsh edges during the hurricane, resulting in more erosion in those areas. Therefore, variations of bed shear stresses, which depend on both wave dissipation and water depth (or local bathymetry), are mainly responsible for the spatial patterns of deposition and erosion in Jamaica Bay during Hurricane Sandy.

One characteristic of storm-generated patterns on the wetland surface (fig. 19) is the paired deposition and erosion patches at local scales (or individual marsh islands). In other words, a patch of deposition on the marsh surface is accompanied by the erosion in adjacent tidal creeks, mudflat, or ponding areas. This could be explained by the preferential trapping of sediment by vegetation in interior marshes and the erosion in nonvegetated areas, supported by measurements of field samples on both ^{234}Thxs and Beryllium-7 (^{7}Be) inventories in the bay (Renfro, 2010).

In some deep bay areas (for example, the southwest area of the Grassy Bay), deposition rather than erosion was caused by Hurricane Sandy (fig. 19). Model results support the observation that the borrow pits such as Grassy Bay could serve as a sink of storm-induced sediment transport, thus limiting sediment transport and deposition on the marsh surface (Rafferty and others, 2011). Moreover, shallow channels inside the bay could also be areas of storm-induced sediment deposition. Previous studies also showed that channel shallowing could reduce Sandy-induced storm-tide magnitude (peak water level) by about 15 percent and increased vegetation frictional drag, which thus increases shallow water wave attenuation (Orton and others, 2015a), eventually promoting sediment deposition.

Averaged morphological change at the 10 marsh islands in Jamaica Bay for vegetated area, mudflat-water area, and all areas is shown in figure 20. For vegetated areas, marsh islands in the western part of the bay were eroded, while the eastern part showed overall deposition. Two isolated small islands, Stony Creek and Duck Point, were largely affected by Hurricane Sandy compared to other marsh islands, especially relatively large-sized marsh islands such as JoCo and Yellow Bar. This indicated that small marsh islands inside the bay are more vulnerable to hurricane-induced disturbance than the larger islands with relatively healthy and contiguous vegetation distribution. In contrast, for mudflat-water areas, morphological change at most marsh islands was small (<2 mm), except for large deposition (about 8 mm) at Ruffle Bar and Little Egg and large erosion (about 6 mm) at East High and JoCo.

Comparing morphological changes caused by Hurricane Sandy between vegetated and mudflat-water areas, the two area types were either totally opposite in change or had large differences. The only exception was Black Bank, where vegetated and mudflat-water areas showed similar accretion. When averaged over vegetated and mudflat-water areas, morphological changes at all marsh islands were less than 5 mm (fig. 20). However, the effect of Hurricane Sandy on different marshes may be different. Taking JoCo as an example, the vegetated area benefited from Sandy, resulting in net accretion, while the

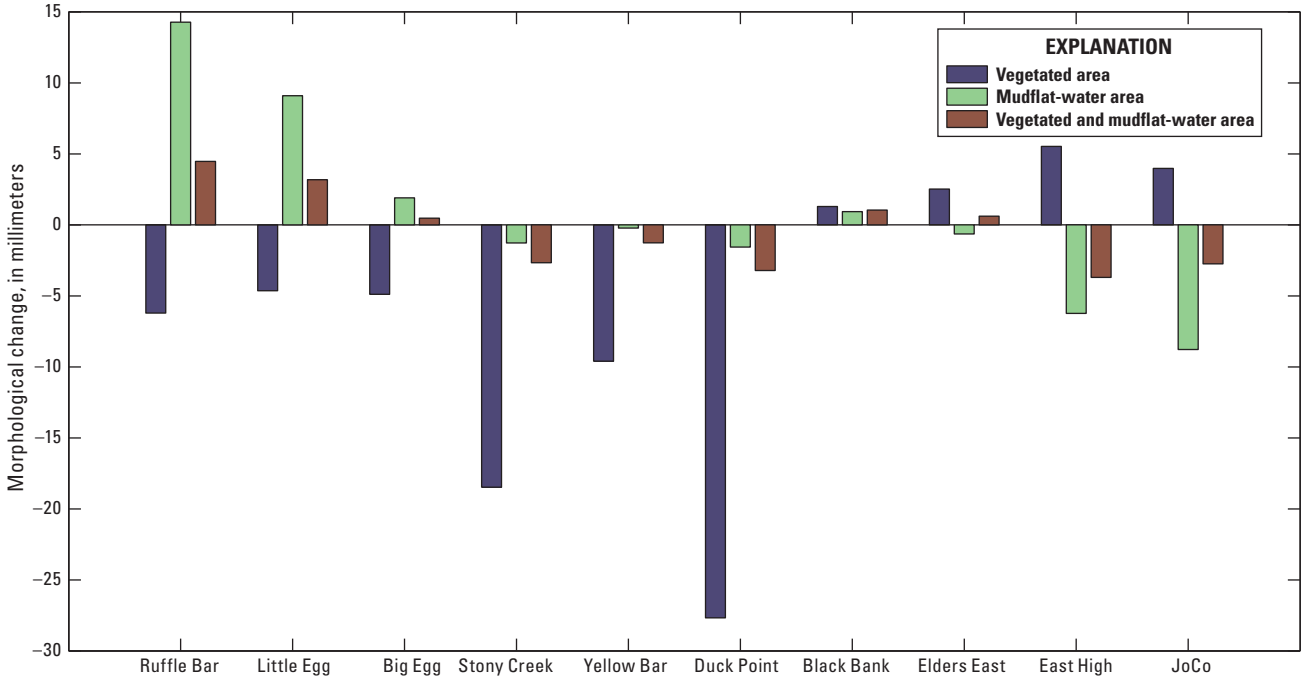

Figure 20. Modeled island-wide morphological change caused by Hurricane Sandy in Jamaica Bay, New York City.

mudflat-water area (for example, inside channels and creeks) lost sediment and showed a negative effect from the hurricane. Overall, Hurricane Sandy was destructive to the marshes in the western part of Jamaica Bay which are being lost or degraded, while the hurricane likely brought more muddy sediment for marsh vertical accretion to the eastern part of the bay. Model results suggest the importance of prioritizing wetland protection and restoration for different marsh islands in the bay.

Long-Term Effects

Scenario results averaged over the vegetated area and mudflat-water area at the 10 marsh islands in Jamaica Bay are shown in figure 21. For the 4-day period, the wetland morphological change in the case without Sandy was close to zero as expected. In comparison, the change with Sandy resulted in erosion in the vegetated area but showed deposition or erosion in mudflat-water areas inside the western part of the bay (figs. 20 and 21). Compared to the west part of the bay, Sandy caused deposition in the vegetated area, but showed erosion (except Black Bank) in the mudflat-water area (figs. 20 and 21). For the 1-year period, both the vegetated and mudflat-water areas on these marsh islands showed either slight deposition or near-zero change, except for the marsh areas of Stony Creek and Duck Point (fig. 21*A*) and the mudflat-water areas of East High and JoCo (fig. 21*B*). Regardless of deposition or erosion on these marsh islands, the difference in morphology between the cases with and without Hurricane Sandy was generally less than 5 mm over the period of 1 year. This suggests that most marshes except those on Stony Creek and Duck Point in Jamaica Bay recovered from the sediment loss due to Hurricane Sandy after 1 year. The morphological change in the case without Sandy was deposition for all marsh areas and most mudflat-water areas. The only exceptions were Big Egg and East High with less erosion (<5 mm) and JoCo with relatively large erosion (>15 mm) (fig. 21*B*). The >5-mm difference of morphological changes between with-Sandy and no-Sandy cases was mostly due to the change induced by Sandy over 4 days, which means the impact of Sandy was still in effect after 1 year at Stony Creek and Duck Point for vegetated areas and at Ruffle Bar, Little Egg, East High, and JoCo for mudflat-water areas (fig. 21).

For the 5-year- and 10-year-period simulations, accretion was prevalent over all marsh areas and most mudflat-water areas, except for Big Egg, East High, and JoCo. The mudflat-water area in Big Egg seems to be in a balanced condition with tiny changes, while those in East High and JoCo showed continued erosion over the years. The difference between with-Sandy and no-Sandy cases became small and was not noticeable on most marsh islands for vegetated and nonvegetated areas, suggesting that the long-term morphological effect of Hurricane Sandy is diminishing. However, in the marsh areas of Stony Creek and Duck Point and the mudflat-water areas of Ruffle Bar and Little Egg, the differences are still prominent (>10 mm). This could imply that the effect of Sandy in some marsh areas may be naturally unrecoverable, especially for those vulnerable small marsh islands in the bay such as Stony Creek and Duck Point. Simulation results also indicated that under normal tide without hurricane conditions, mudflat and creek areas on marsh islands such as East High and JoCo inside the eastern part of the bay appear to be unable to receive sediment delivered from the ocean through Rockaway Inlet or from the bay bottom, and the marsh vertical accretion tended to be at the expense of mudflat or creek bank erosion. Frequent nor'easters or infrequent large hurricanes could help salt marshes on these islands enhance their morphological stability.

The long-term morphological change in Jamaica Bay is more dynamic in channels than that on marshes. In addition, more changes appeared in the western part of the bay than in the eastern part of the bay. As shown in the difference maps (fig. 22) with a small scale in the color bar, the entire bay is affected, with more complex and dynamic patterns in channels and in the western part of the bay. For JoCo, Hurricane Sandy induced not only more deposition in the vegetated area, but also more erosion in channels and creeks which are around and inside the marsh island. This trend changes little over the years.

The model results shown in figures 18–19 and 22 indicate that Sandy-induced marsh vertical accretion by deposition is most likely detected and preserved in relatively healthy salt marshes on marsh islands inside the eastern part of the bay. In contrast, the Sandy-induced vertical accretion is hardly detectable in the salt marshes inside the western part of the bay because of the storm-induced erosion. These results are consistent with results from previous studies that indicate that the signal and preservation of hurricane sediment deposition are determined by the track, landfall location, and intensities of hurricanes, the proximity to the ocean or barrier islands, and the topo-bathymetric characteristics of the subtidal bay and intertidal salt marshes (Bentley and others, 2002; Scileppi and Donnelly, 2007).

Effects of Hypothetical Hurricanes

When approaching Jamaica Bay, Sandy-like hurricanes are west-moving, while Irene-like hurricanes are north-moving. Only the immediate effects (4 days) on vegetated areas in the 10 marsh islands are discussed here.

Sandy-Like Hurricanes

First of all, the morphology patterns for all Sandy-like hurricanes did not change with different tracks and intensities, and only varied in magnitude. Hurricane SA is shifted closer to Jamaica Bay and is assumed to have a more severe impact (table 5). In fact, SA did induce more changes at six marsh

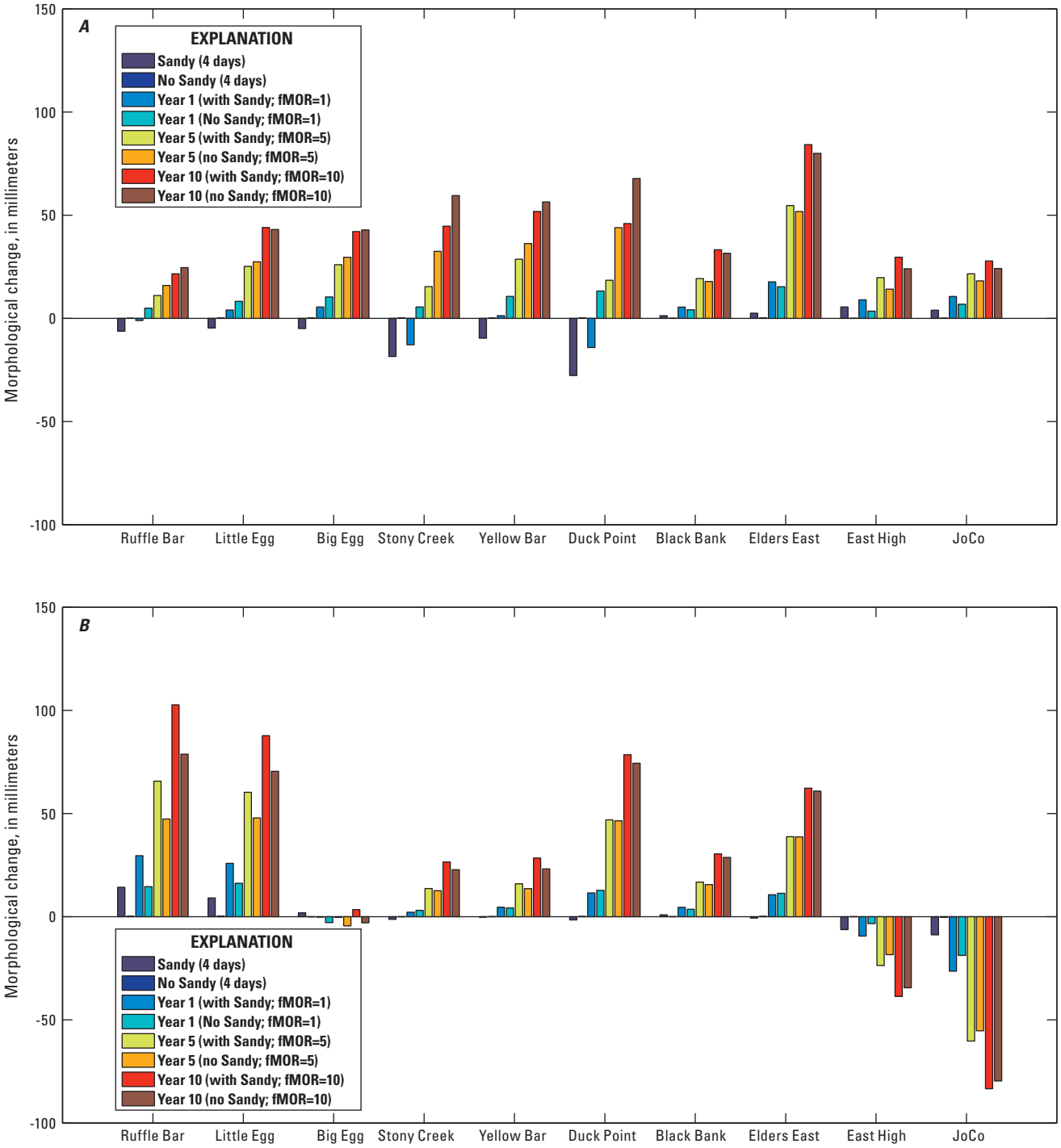

Figure 21. Island-wide morphological change in *A*, vegetated area and *B*, mudflat-water area in Jamaica Bay with and without Hurricane Sandy during the event (4 days) and for 1, 5, and 10 years.

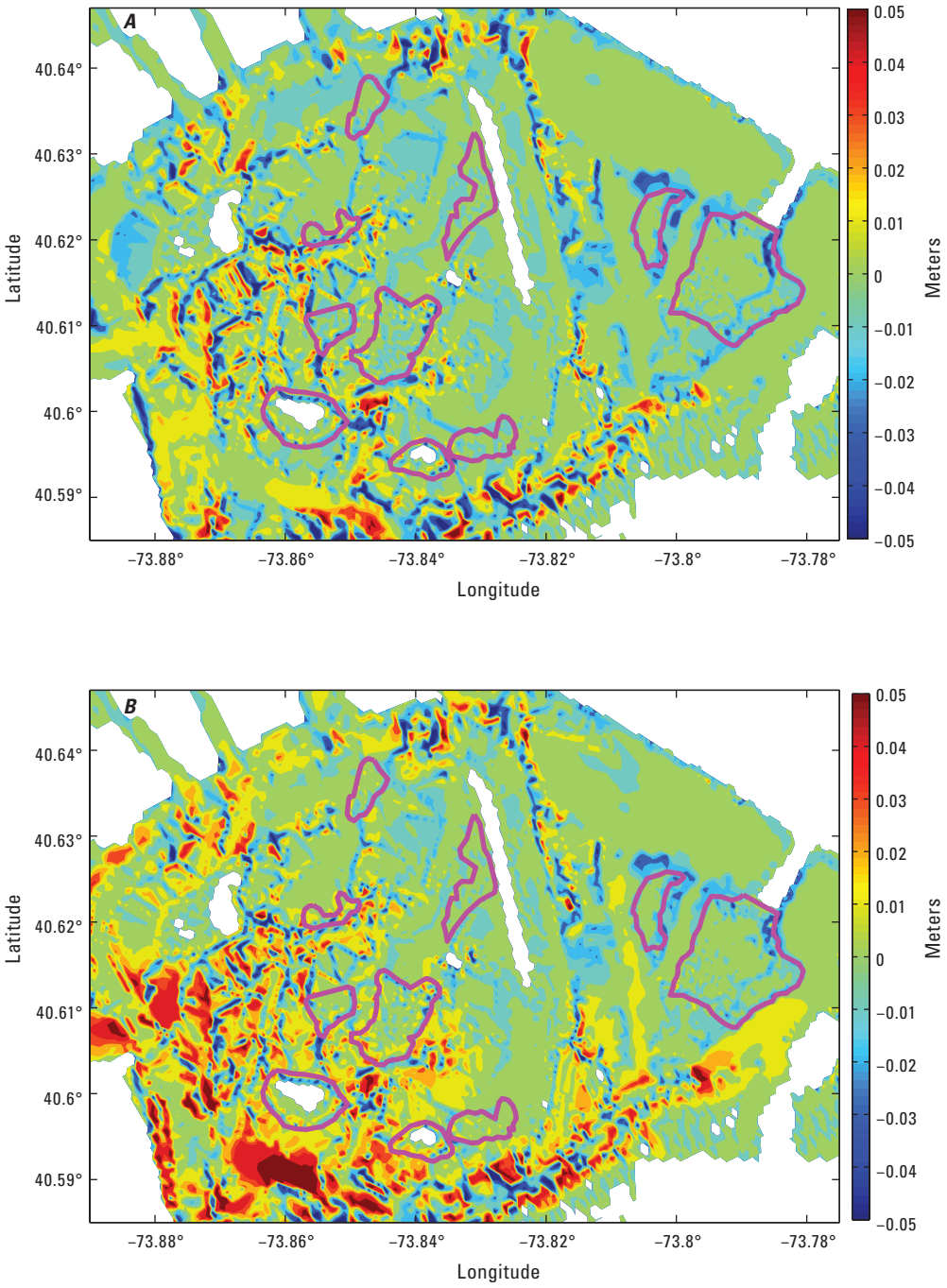

Figure 22. Modeled spatial bay-wide morphological changes caused by Hurricane Sandy in Jamaica Bay, New York City, *A*, for 1 year (short-term) and *B*, for 10 years (decadal).

islands and caused maximum erosion (>35 mm) at Duck Point, but still showed less morphological changes at four of the marsh islands (Black Bank, Elder East, East High, and JoCo, fig. 23*A*). Similar situations occurred during Hurricanes SB and SC. It is not the worst scenario that hurricanes like Sandy directly hit Jamaica Bay. Among track-varying cases, SB induced maximum erosion only on two marsh islands—Big Egg and Stony Creek. When comparing SA with SC, SA caused more morphological change than SC on most of the marsh islands except Big Egg, suggesting a hurricane with landfall location to the west and south of Jamaica Bay tends to have more effect on morphology than those with landfall location to the east of the bay. For different storm intensities, the trend appeared much simpler. In general, the higher the wind intensity, the more morphological change on these marsh islands in Jamaica Bay, except for Big Egg and Stony Creek (fig. 23*B*).

Irene-Like Hurricanes

Unlike Sandy-like hurricanes, Irene-like hurricanes caused erosion on all marsh islands except JoCo in Jamaica Bay (fig. 23*C*). For the four marsh islands where deposition resulted from Sandy-like hurricanes, Irene-like hurricanes were more destructive than the Sandy-like storms. For the rest of the six marsh islands, Irene-like hurricanes induced less erosion than Hurricane Sandy, except for the enhanced Irene, IC, which induced more erosion than Sandy. Comparing the more offshore case IA with the more inland case IB, IB was more destructive to all marsh islands than IA, which indicated that with the same intensities, hurricanes passing to the west are more dangerous to Jamaica Bay than those passing to the east. Finally, it is found that among all hypothetical hurricane scenarios, the six marsh islands in the western part of the bay always lost sediment due to erosion in vegetated areas. In other words, the vegetated areas in the western part were more vulnerable to the hurricane impact than those in the eastern part of the bay.

Conclusions

Hurricane Sandy, which made landfall along the east coast of the United States on October 29, 2012, provides a critical opportunity for studying the effects of hurricanes on sediment transport, deposition, erosion, and associated morphological changes in Jamaica Bay, New York City. The Delft3D model suite was applied to assess and predict hydrodynamics and sediment transport driven by Hurricane Sandy and hypothetical hurricanes in Jamaica Bay. The reasonable agreement of modeled wave parameters, water levels, and morphological change with field measurements during Hurricane Sandy indicated good model performance under hurricane conditions.

After calibration and validation of the model system, numerical simulations under a series of scenarios were carried out to investigate the short-term and long-term effects of Hurricane Sandy and the immediate effects of hypothetical hurricanes on the wetland morphology in Jamaica Bay. For the immediate effect of Hurricane Sandy, the morphological change was extremely complex and more dynamic in the western part of Jamaica Bay (for example, Yellow Bar) than the eastern part (for example, JoCo). Many erosion/accretion patches were generated by local hydrodynamics. For vegetated areas, six wetlands in the western part of the bay were eroded, while four wetlands in the eastern part showed deposition. After 1 year, most wetlands in Jamaica Bay recovered from the sediment loss due to Hurricane Sandy, while the impact of Sandy was still in effect. For the 5-year and 10-year periods, the long-term morphology in Jamaica Bay has greater variability in channels than on wetlands, where hurricane effects could hardly be detected island-wide. Accretion was prevalent over wetlands in Jamaica Bay over the long periods with transport of sediment from external and internal sources by way of normal tide and infrequent winter storms. The long-term effect of Sandy is diminished, while some vulnerable salt marshes on small islands such as Stony Creek and Duck Point still cannot recover. For some salt marshes like JoCo, the storm impact has two aspects; that is, Sandy induced not only more deposition in the vegetated area, but also more erosion in channels and creeks of the marsh island.

The basic morphology patterns caused by Sandy-like hurricanes would not change with different tracks and intensities and a Sandy-like hurricane directly hitting Jamaica Bay would not be the worst scenario. Hurricanes land-falling to the west and south of the bay would have more effect on the morphology than those to the east of the bay. Higher wind intensities would induce more morphological change in the wetlands of Jamaica Bay. Irene-like hurricanes would cause erosion in all wetlands (except JoCo) in Jamaica Bay. With the same wind intensities, hurricanes passing to the west would be more destructive to salt marshes in Jamaica Bay than those passing to the east. Among all hypothetical hurricane scenarios, the vegetated areas in the western part of the bay appeared to be more vulnerable to the hurricane impacts than those in the eastern part.

Previous studies found that the primary causes of marsh loss in an urbanized setting such as Jamaica Bay are biogeochemical and not geophysical (for example, Kolker, 2005). The findings in our study suggest that large-scale, infrequent, and intense hurricanes can enhance marsh accretion and erosion depending on storm features and wetland characteristics. Considering the predicted increased frequency, intensity, and duration of future hurricanes, it is hypothesized that hurricanes may expedite the disappearance of the marsh islands in the western part of Jamaica Bay if no further protection and restoration actions are taken. Our study also found that the larger the vegetated marsh island size, the less the degree of storm-induced erosion, suggesting that marsh continuity and land percentage (total vegetated area to total island area) are important in restoring marshes in Jamaica Bay.

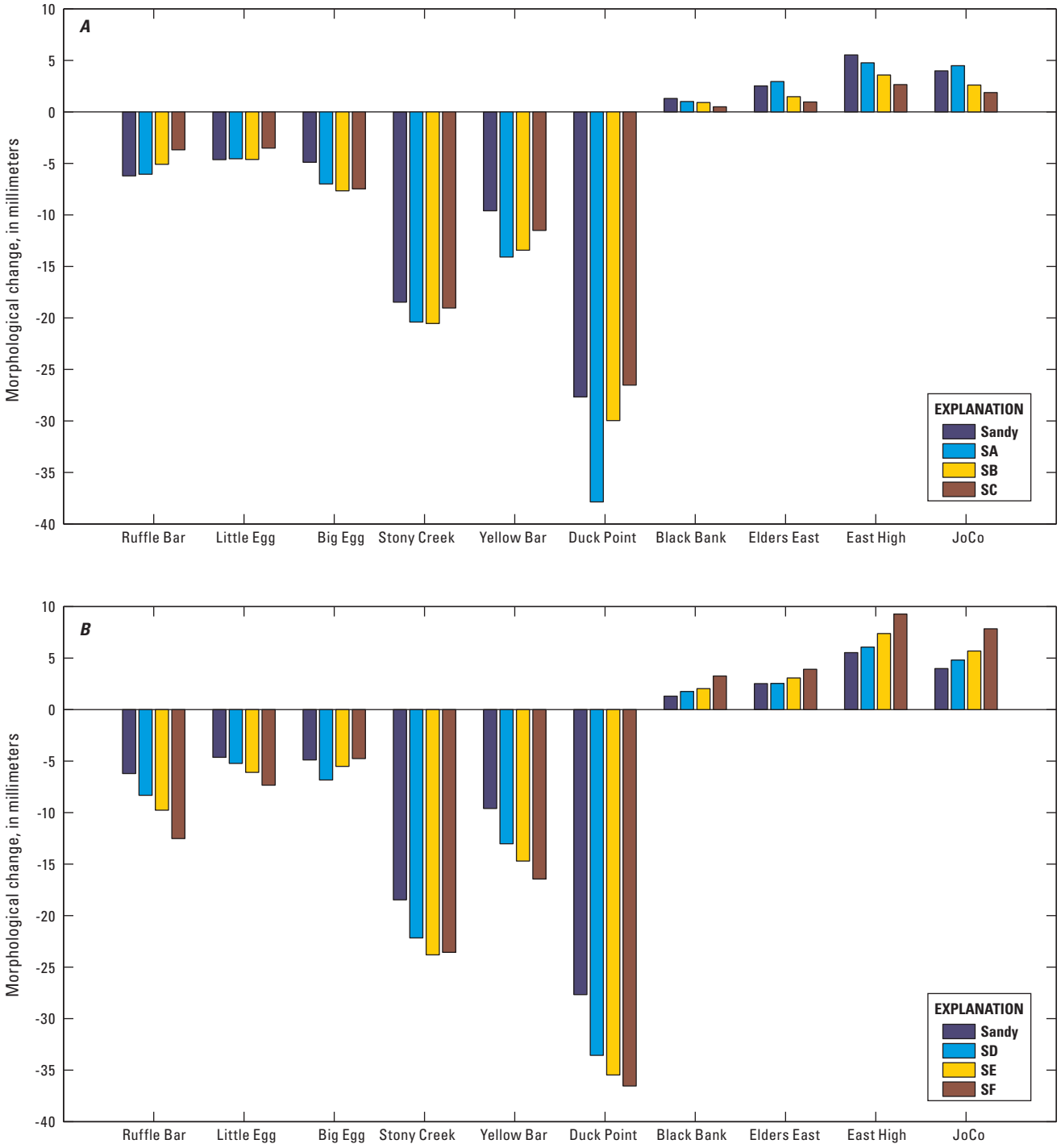

Figure 23. Modeled island-wide wetland morphological change in Jamaica Bay, New York City, due to difference in *A*, track and *B*, intensity of Sandy-like hurricanes and *C*, track and intensity of Irene-like hurricanes.

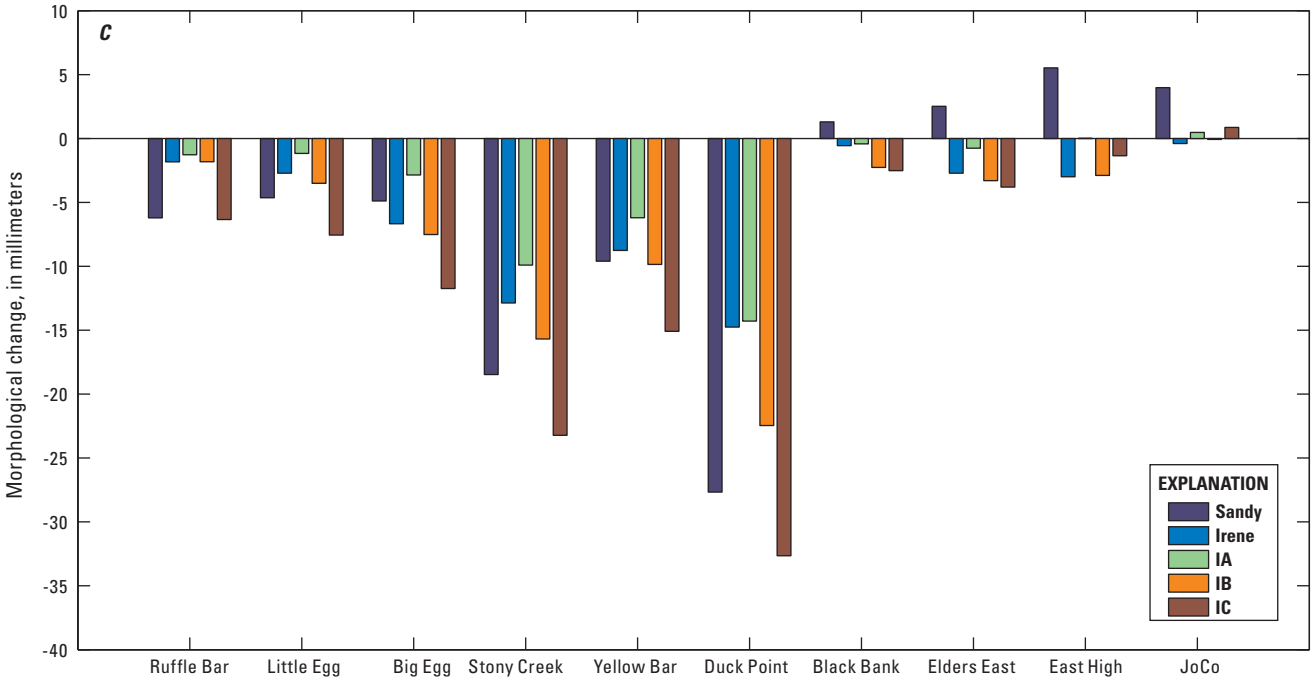

Figure 23. Modeled island-wide wetland morphological change in Jamaica Bay, New York City, due to difference in *A*, track and *B*, intensity of Sandy-like hurricanes and *C*, track and intensity of Irene-like hurricanes.—Continued

From this study, the following conclusions can be made:

1. The validated numerical model has revealed the spatial patterns of wetland morphology in Jamaica Bay under hurricanes, in the order of large to small, by storm feature (for example, intensity), geomorphological setting (for example, distance to storm track or bathymetry), and vegetation distribution.

2. Hurricane-generated sediments in the bay and marsh islands are mainly from reworking of bay bottom resuspension and marsh edge erosion, rather than from the ocean by way of Rockaway Inlet.

3. Modeling localized morphology change needs high-resolution topographic and bathymetric data to resolve small scale landscape features such as small tidal creeks within marsh islands. In this study, ≤10-m resolution is required to identify the breach along the West Pond trail in the Jamaica Bay Wildlife Refuge.

4. Hurricane-generated bay and wetland morphological changes are spatially discrete and local in nature rather than nearly uniform responses such as beach and dunes.

5. Local variations of bed shear stresses from hurricane waves are the main driver of the localized bay and wetland morphology change.

6. The deep channels and Grassy Bay serve as a major sink of hurricane-mobilized sediments, similar to the sediment pathway under normal tide and winter storm conditions.

7. Because marsh resilience is dependent upon sediment supply (Fagharazzi and others, 2013a; Twilley and others, 2016), and large storm-reworked sediments (either local or from ocean) are transported to deep channels or borrow pits as sinks, more sediment supply from external sources would be needed for restoration of wetlands in Jamaica Bay.

There are some model limitations in this study. First, the grid resolution in Jamaica Bay is not fine enough to resolve detailed features of some wetlands (for example, small creeks <10 m in width in JoCo), especially in the basin-wide domain for long-term simulations with a grid size of 50 m. Second, the calibration and validation of the model parameters are still very limited due to lack of observed data in Jamaica Bay, such as wave parameters, current, and suspended sediment concentration. For example, measurements of wave characteristics from only one offshore buoy nearest Jamaica Bay were used in the wave model. More field measurements would improve the model performance substantially. Third, vegetation properties were fixed, and flow invariant constant values of Manning's

coefficient for certain types of vegetation were used in the Delft3D-FLOW model, potentially underestimating vegetation effect. In reality, the relevant vegetation properties vary seasonally and yearly. If vegetation could vary with morphological change over a year with different seasons and even include vegetation mortality under exceeded inundation and salinity tolerance/thresholds for long-term cases, the model would be more realistic. Additionally, vegetation was assumed to be rigid cylindrical structures of small diameter. But, in reality, plants tend to bend as water depth and flow velocity increase during storms and especially hurricanes (Zhao and Chen, 2014, 2016), resulting in reduced plant resistance to flow, and enhancing sediment transport further into the interior wetland areas. Vegetation may be damaged and need a recovery period before resuming pre-storm characteristics. Therefore, a dynamic Manning's coefficient as a function of flow conditions and vegetation characteristics should be included in future hurricane-wetland morphology modeling because of the highly spatial heterogeneity in wave energy dissipation affecting sediment transport at local scales due to large hurricanes. Furthermore, vegetation properties should be used in the hurricane wave model (Zhao and Chen, 2014, 2016).

Fourth, with the application of morphological acceleration factor fMOR, a 1-year simulation can provide results for a period of multiple years. However, it is not easy to get 1-year representative winds from multiple-year winds. In this study, the first-year winds were used to represent the 5-year or 10-year winds, which may introduce errors. Fifth, the coupled model is sensitive to model parameters of critical shear stress, erodibility coefficient, and settling velocity as demonstrated in other Delft3D morphology studies (George and others, 2012; Liu and others, 2015; Liu, 2016). As field data and literature on these parameters are limited, we calibrated the critical shear stress for different land-cover types. In reality, the variability of sediment texture (type, density) will cause variations of bed erodibility, settling velocity, and critical shear stress in space and time, and ultimately different morphological responses. Future field work is needed to examine the spatial and temporal variability in these parameters as a function of sediment texture.

The coupled hurricane-wetland morphology modeling system has been demonstrated by this study to be capable of assisting coastal resource managers in the planning and implementation of various restoration efforts. Particularly, we suggest that the validated model may benefit sediment operations, such as helping managers decide the location, area, depth, and grain size of the placement of dredged materials from the Harbor Deepening Project and the optimal height, density, and planting elevation for maximum inorganic sediment trapping in Jamaica Bay, New York City.

References

American Littoral Society, 2012, Assessing the impacts of Hurricane Sandy on coastal habitats. Final report for the National Fish and Wildlife Foundation, accessed January 25, 2017, at http://www.crssa.rutgers.edu/projects/coastal/sandy/doc/ALS%20NFWF%20Final%20Assessment%20Report%20121712.pdf.

Baptist, M.J., 2005, Modeling floodplain biogeomorphology: Ph.D. thesis, Delft University of Technology.

Benotti, M.J., Abbene, Michele, and Terracciano, S.A., 2007, Nitrogen loading in Jamaica Bay, Long Island, New York: Predevelopment to 2005: U.S. Geological Survey Scientific Investigations Report 2007–5051, 17 p., accessed December 30, 2016, at https://pubs.usgs.gov/sir/2007/5051/.

Bentley, S.J., Keen, R.R., Blain, C.A., and Vaughan, W.C., 2002, The origin and preservation of a major hurricane event bed in the northern Gulf of Mexico: Hurricane Camille, 1969: Marine Geology, v. 186, p. 423–446.

Black, F.R., 1981, Jamaica Bay: A history, Gateway National Recreation Area, New York, New Jersey: Washington, D.C., National Park Service.

Blake, E.S., Kimberlain, T.B., Berg, R.J., Cangialosi, J.P., and Beven, J.L., 2013, Tropical cyclone report, Hurricane Sandy (AL182012): National Hurricane Center, accessed January 18, 2017, at http://www.nhc.noaa.gov/data/tcr/AL182012_Sandy.pdf.

Brandon, C.M., Woodruff, J.D., Donnelly, J.P., and Sullivan, R.M., 2014, How unique was Hurricane Sandy? Sedimentary reconstructions of extreme flooding from New York Harbor: Scientific Reports, v. 4, article number 7366. DOI:10.1038/srep07366.

Brown, J.L., 1981, Jamaica Bay: A history, Gateway National Recreation Area, New York, New Jersey: Washington, D.C., National Park Service, U.S. Department of Interior.

Bunya, S., Dietrich, J.C., Westerink, J.J., Ebersole, B.A., Smith, J.M., Atkinson, J.H., Jensen, R., Resio, D.T., Luettich, R.A., Dawson, C., Cardone, V.J., Cox, A.T., Powell, M.D., Westerink, H.J., and Roberts, H.J., 2010, A high-resolution coupled riverine flow, tide, wind, wind wave, and storm surge model for southern Louisiana and Mississippi. Part I: Model development and validation: Monthly Weather Review, v. 138, p. 345–377.

Cahoon, D.R., 2006, A review of major storm impacts on coastal wetland elevations: Estuaries and Coasts, v. 29, p. 889–898.

Cahoon, D.R., Lynch, J.C., and Hensel, P.F., 2006, Monitoring salt marsh elevation: A protocol for the long-term coastal ecosystem monitoring program at Cape Cod National Seashore: U.S. Geological Survey, Patuxent Wildlife Research Center, last accessed January 18, 2017, at https://www.nps.gov/caco/learn/nature/upload/CACO-Salt-Marsh-Elevation-Monitoring-Protocol-Final.pdf.

Cahoon, D.R., Reed, D.J., Day, J.W., Steyer, G.D., Boumans, R.M., Lynch, J.C., McNally, D., and Latif, N., 1995, The influence of Hurricane Andrew on sediment distribution in Louisiana coastal marshes: Journal of Coastal Research Special Issue, v. 21, p. 280–294.

Chen, Q., Wang, L., and Tawes, R., 2008, Hydrodynamic response of northeastern Gulf of Mexico to hurricanes: Estuaries and Coasts, v. 31, no. 6, p. 1098–1116.

Chen, X., Chen, Q., Zhan, J., and Liu, D., 2016, Numerical simulations of wave propagation over a vegetated platform: Coastal Engineering, v. 110, p. 64–75.

Chmura, G.L., and Kosters, E.C., 1994, Storm deposition and ^{137}Cs accumulation in fine-grained marsh sediments of the Mississippi Delta plain: Estuarine, Coastal and Shelf Science, v. 39, p. 33–44.

Dalrymple, R.A., Kirby, J.T., and Hwang, P.A., 1984, Wave diffraction due to areas of energy dissipation: Journal of Waterways, Ports, Harbours and Coastal Engineering, v. 110, p. 67–79.

Danielson, J.J., Poppenga, S.K., Brock, J.C., Evans, G.A., Tyler, D.J., Gesch, D.B., Thatcher, C.A., and Barras, J.A., 2016, Topobathymetric elevation model development using a new methodology: Coastal National Elevation Database: Journal of Coastal Research, Special Issue 76, p. 75–89.

Deltares, 2017, Delft3D open source community, last accessed January 18, 2017, at http://oss.deltares.nl/web/delft3d.

De Vriend, H.J., Zyserman, J., Nicholson, J., Roelvink, J.A., Pechon, P., and Southgate, H.N., 1993, Medium-term 2DH coastal area modeling: Coastal Engineering, v. 21, p. 193–224.

Dietrich, J.C., Westerink, J., Kennedy, A., Smith, J., Jensen, R., Zijlema, M., Holthuijsen, L., Dawson, C., Luettich, R., Jr., and Powell, M., 2011, Hurricane Gustav (2008) waves and storm surge: Hindcast, synoptic analysis, and validation in southern Louisiana: Monthly Weather Review, v. 139, no. 8, p. 2488–2522.

Fagherazzi, S., Mariotti, G., Wiberg, P.L., and McGlathery, K.J., 2013a, Marsh collapse does not require sea level rise: Oceanography, v. 26, p. 70–77.

Fagherazzi, S., Wiberg, P.L., Temmerman, S., Struyf, E., Zhang, Y., and Raymond, P.A., 2013b, Fluxes of water, sediments, and biogeochemical compounds in salt marshes: Ecological Processes, v. 2, last accessed January 3, 2017, at https://ecologicalprocesses.springeropen.com/articles/10.1186/2192-1709-2-3.

Federal Emergency Management Agency, 2014, Region II Coastal Storm Surge Study: Overview: Washington, D.C., 11 p.

George, D.A., Gelfenbaum, G., and Stevens, A.W., 2012, Modeling the hydrodynamic and morphologic response of an estuary restoration: Estuaries and Coasts, v. 35, p. 1510–1529.

Goodbred, S.L., and Hine, A.C., 1995, Coastal storm deposition: Salt-marsh response to a severe extratropical storm, March 1993, west-central Florida: Geology, v. 23, no. 8, p. 679–682.

Harmon, D., 2006, People, places, and parks: Proceedings of the 2005 George Wright Society Conference on Parks, Protected Areas, and Cultural Sites: Hancock, Mich., The George Wright Society.

Hartig, E.K., Gornitz, V., Kolker, A., Mushacke, F., and Fallon, D., 2002, Anthropogenic and climatic change impacts on salt marshes of Jamaica Bay, New York City: Wetlands, v. 22, no. 1, p. 71–89.

Horton, R., Little, C., Gornitz, V., Bader, D., and Oppenheimer, M., 2015, New York City Panel on Climate Change 2015 Report Chapter 2: Sea Level Rise and Coastal Storms: Annals of the New York Academy of Sciences, v. 1336, p. 36–44.

Hu, K., Ding, P., Wang, Z., and Yang, S., 2009, A 2D/3D hydrodynamic and sediment transport model for the Yangtze Estuary, China: Journal of Marine Systems, v. 77, p. 114–136.

Hu, K., Chen, Q., and Kimball, K.S., 2012, Consistency in hurricane surface wind forecasting: An improved parametric model: Natural Hazards, v. 61, p. 1029–1050.

Hu, K., Chen, Q., and Wang, H., 2015, A numerical study of vegetation impact on reducing storm surge by wetlands in a semi-enclosed estuary: Coastal Engineering, v. 95, p. 66–76.

Kolker, A.S., 2005, The impacts of climate variability and anthropogenic activities on salt marsh accretion and loss on Long Island: Stony Brook, N.Y., Stony Brook University, Ph.D. dissertation, 261 p.

Lesser, G.R., Roelvink, J.A., Van Kester, J.A.T.M., and Stelling, G.S., 2004, Development and validation of a three-dimensional morphological model: Coastal Engineering, v. 51, p. 883–915.

Lindemer, C.A., Plant, N.G., Puleo, J.A., Thompson, D.M., and Wamsley, T.V., 2010, Numerical simulation of a low-lying barrier island's morphological response to Hurricane Katrina: Coastal Engineering, v. 57, p. 985–995.

Liu, K., 2016, Numerical simulations of wind effects on wave nonlinearity and hurricane-induced sediment transport: Baton Rouge, La., Louisiana State University, Ph.D. dissertation.

Liu, K., Chen, Q., Hu, K., and Xu, K., 2015, Numerical simulation of sediment deposition and erosion on Louisiana Coast during Hurricane Gustav, *in* Proceedings of the Coastal Sediments 2015 conference, May 11–15, 2015, San Diego, Calif.

Loder, N.M., Irish, J.L., Cialone, M.A., and Wamsley, T.V., 2009, Sensitivity of hurricane surge to morphological parameters of coastal wetlands: Estuarine, Coastal and Shelf Science, v. 84, p. 625–636.

McKee, K.L., and Cherry, J.A., 2009, Hurricane Katrina sediment slowed elevation loss in subsiding brackish marshes of the Mississippi River delta: Wetlands, v. 29, p. 2–15.

Mendez, F.J., and Losada, I.J., 2004, An empirical model to estimate the propagation of random breaking and nonbreaking waves over vegetation fields: Coastal Engineering, v. 51, p. 103–118.

Miles, T., Seroka, G., Kohut, J., Schofield, O., and Glenn, S., 2015, Glider observations and modeling of sediment transport in Hurricane Sandy: Journal of Geophysical Research: Oceans, v. 120, last accessed January 3, 2017, at http://onlinelibrary.wiley.com/doi/10.1002/2014JC010474/pdf.

Miselis, J.L., Andrews, B.D., Nicholson, R.S., Defne, Z., Ganju, N.K., and Navoy, A., 2015, Evolution of Mid-Atlantic coastal and back-barrier estuary environments in response to a hurricane: Implications for barrier-estuary connectivity: Estuaries and Coasts, last accessed January 3, 2017, at http://link.springer.com/article/10.1007/s12237-015-0057-x.

Mukai, A.Y., Westerink, J.J., Luettich, R.A., Jr., and Mark, D., 2002, Eastcoast 2001, a tidal constituent database for Western North Atlantic, Gulf of Mexico, and Caribbean Sea: U.S. Army Corps of Engineers Technical Report ERDC/CHL TR-02-24 [variously paged].

Nardin, W., and Edmonds, D.A., 2014, Optimum vegetation height and density for inorganic sedimentation in deltaic marshes: Nature Geoscience, v. 7, p. 722–726.

National Oceanic and Atmospheric Administration, 2010, GEODAS (GEOphysical DAta System): National Geophysical Data Center, National Oceanic and Atmospheric Administration, accessed January 25, 2017, at http://www.ngdc.noaa.gov/mgg/geodas/geodas.html.

New York City Department of Environmental Protection, 2007, Jamaica Bay watershed protection plan: Volume II—The plan, last accessed January 3, 2017, at http://www.esf.edu/glrc/documents/Jamaica%20Bay%20Watershed%20Protection%20Plan%20volume%202.pdf.

New York State Department of Environmental Conservation, 2017, Tidal Wetlands Categories, last accessed January 26, 2017, at http://www.dec.ny.gov/lands/5120.html.

Nordenson, C.S., Alexander, K., Alessi, D., and Sands, E., 2015, Jamaica Bay plant catalog: The City College of New York, 99 p., accessed January 3, 2017, at http://structuresofcoastalresilience.org/wp-content/uploads/2014/10/REF-02-Jamaica-Bay-Plant-Catalog_sm.pdf.

Nyman, J.A., Crozier, C.R., and DeLaune, R.D., 1995, Roles and patterns of hurricane sedimentation in an estuarine marsh landscape: Estuarine, Coastal and Shelf Science, v. 40, p. 665–679.

Orton, P., Georgas, N., Blumberg, A., and Pullen, J., 2012, Detailed modeling of recent severe storm tides in estuaries of the New York City region: Journal of Geophysical Research, v. 117, C09030, last accessed January 3, 2017, at http://onlinelibrary.wiley.com/doi/10.1029/2012JC008220/epdf.

Orton, P., Hall, T., Talke, S., Blumberg, A., Georgas, N., and Vinogradov, S., 2016, A validated tropical-extratropical flood hazard assessment for New York Harbor: Journal of Geophysical Research, v. 121, p. 8904–8929.

Orton, P., Talke, S.A., Jay, D.A., Yin, L., Blumberg, A.F., Georgas, N., Zhao, H., Roverts, H., and MacManus, K., 2015a, Channel shallowing as mitigation of coastal flooding: Journal of Marine Science and Engineering, v. 3, p. 654–673.

Orton, P., Vinogradov, S., Georgas, N., Blumberg, A., Lin, N., Gornitz, V., Little, C., Jacob, K., and Horton, R., 2015b, New York City Panel on Climate Change 2015 Report Chapter 4: Dynamic Coastal Flood Modeling. Annals of the New York Academy of Sciences, v. 1336, p. 56–66.

Partheniades, E., 1965, Erosion and deposition of cohesive soils: Journal of the Hydraulics Division, v. 91, no. 1, p. 105–139.

Rafferty, P., Castagna, J., and Adamo, D., 2011, Building partnerships to restore an urban marsh ecosystem at Gateway National Recreation Area: Park Science, v. 27, no. 3.

Ranasinghe, R., Swinkels, C., Luijendijk, A., Roelvink, D., Bosboom, J., Stive, M., and Walstra, D., 2011, Morphodynamic upscaling with the MORFAC approach: Dependencies and sensitivities: Coastal Engineering, v. 58, p. 806–811.

Renfro, A.A., 2010, Particle-reactive radionuclides (^{234}Th, ^{7}Be and ^{210}Pb) as tracers of sediment dynamics in an urban coastal lagoon (Jamaica Bay, NY): Stony Brook, N.Y., Stony Brook University, Ph.D. dissertation, 294 p.

Renfro, A., Cochran, J.K., Hirschberg, D.J., and Goodbred, S.L., 2010, Natural radionuclides (^{234}Th, ^{7}Be and ^{210}Pb) as indicators of sediment dynamics in Jamaica Bay, New York: Fort Collins, Colo., Natural Resource Technical Report NPS/NERO/NRTR—2010/324.

Scileppi, E., and Donnelly, J.P., 2007, Sedimentary evidence of hurricane strikes in western Long Island, New York: Geochemistry Geophysics Geosystems, v. 8, no. 6, p. 1–25.

Smith, J.E., Bentley, S.J., Snedden, G.A., and White, C., 2015, What role do hurricanes play in sediment delivery to subsiding river deltas?: Scientific Reports 5, article number 17582, DOI: 10.1038/srep17582.

Smith, J.M., and Anderson, M.E., 2014, Limits of wetland wave dissipation, *in* Lynett, P., ed., Proceedings of 34th Conference on Coastal Engineering: Seoul, South Korea, 10 p., last accessed January 3, 2017, at http://dx.doi.org/10.9753/icce.v34.waves.18.

Sopkin, K.L., Stockdon, H.F., Doran, K.S., Plant, N.G., Morgan, K.L.M., Guy, K.K., and Smith, K.E.L., 2014, Hurricane Sandy: Observations and analysis of coastal change: U.S. Geological Survey Open-File Report 2014–1088, 54 p., last accessed January 3, 2017, at http://dx.doi.org/10.3133/ofr20141088.

Steinberg, N., Suszkowski, D.J., Clark, L., and Way, J., 2004, Health of the harbor: The first comprehensive look at the state of the estuary: New York, Hudson River Foundation, 82 p.

Stockdon, H.F., Sallenger, A.H., Holman, R.A., and Howd, P.A., 2007, A simple model for the spatially-variable coastal response to hurricanes: Marine Geology, v. 238, p. 1–20.

Swanson, R.L., and Wilson, R.E., 2008, Increased tidal ranges coinciding with Jamaica Bay development contribute to marsh flooding: Journal of Coastal Research, v. 24, p. 1565–1569.

Talke, S.A., Orton, P., and Jay, D.A., 2014, Increasing storm tides in New York Harbor, 1844–2013: Geophysical Research Letters, v. 41, p. 3149–3155, last accessed January 3, 2017, at http://onlinelibrary.wiley.com/doi/10.1002/2014GL059574/abstract.

Temmerman, S., Bouman, T.J., Govers, G., Wang, Z.B., De Vries, M.B., and Herman, P.M.J., 2005, Impact of vegetation on flow routing and sedimentation patterns: Three-dimensional modeling for a tidal marsh: Journal of Geophysical Research, v. 110, p. 1–18.

Transactions of the Linnaean Society of New York, 2007, Natural history of New York City's parks and Great Gull Island: New York City, N.Y., The Linnaean Society of New York, National Parks Conservation Association, City of New York Parks & Recreation, 180 p., last accessed January 3, 2017, at http://linnaeannewyork.org/information/images/Transactions_X.pdf.

Turner, R.E., Baustian, J.J., Swenson, E.M., and Spicer, J.S., 2006, Wetland sedimentation from Hurricanes Katrina and Rita: Science, v. 314, p. 449–452.

Tweel, A.W., and Turner, R.E., 2012, Landscape-scale analysis of wetland sediment deposition from four tropical cyclone events: PlOS ONE, v. 7, no. 11, e50528.

Twilley, R.R., Bentley, S.J., Chen, Q., Edmonds, D.A., Hagen, S.C., Lam, N., Willson, C.S., Xu, K., Braud, D.W., Peels, R.H., and McCall, A., 2016, Co-evolution of wetland landscapes, flooding and human settlement in the Mississippi River Deltaic Plan: Sustainability Science, last accessed January 3, 2017, at http://link.springer.com/article/10.1007/s11625-016-0374-4.

U.S. Fish & Wildlife Service, 2017, National Wetlands Inventory, last accessed January 26, 2017, at https://www.fws.gov/wetlands/data/wetland-codes.html.

U.S. Department of Agriculture, Natural Resources Conservation Service, 2017, Plants Database, last accessed January 26, 2017, at http://plants.usda.gov/java/factSheet.

Van Rijn, L.C., 1993, Principles of sediment transport in rivers, estuaries and coastal seas: Amsterdam, Aqua Publications.

Van Rijn, L.C., Roelvink, J.A., and Horst, W.T., 2000, Approximation formulae for sand transport by currents and waves and implementation in DELFT-MOR: The Netherlands, Delft Hydraulics, Technical Report Z3054.40.

Van Rijn, L.C., Walstra, D., Grasmeijer, B., Sutherland, J., Pan, S., and Sierra, J., 2003, The predictability of cross-shore bed evolution of sandy beaches at the time scale of storms and seasons using process-based profile models: Coastal Engineering, v. 47, p. 295–327.

Vogelmann, J.E., Howard, S.M., Yang, L., Larson, C.R., Wylie, B.K., and Van Driel, J.N., 2001, Completion of the 1990's National Land Cover Data Set for the conterminous United States: Photogrammetric Engineering and Remote Sensing, v. 67, p. 650–662.

Wang, J.D., Swain, E.D., Wolfert, M.A., Langevin, C.D., James, D.E., and Telis, P.A., 2007, Application of FTLOADDS to simulate flow, salinity, and surface-water stage in the southern Everglades, Florida: U.S. Geological Survey Scientific Investigations Report 2007–5010, 112 p.

Wang, Y., Christiano, M., and Traber, M., 2010, Mapping salt marsh in Jamaica Bay and terrestrial vegetation in Fire Island National Seashore using QuickBird satellite data, *in* Wang, Y., ed., Remote sensing of coastal environments: CRC Press, p. 191–208.

Wigand, C., Roman, C.T., Davey, E.W., Stolt, M.H., Johnson, R.L., Hanson, A., Watson, E.B., Moran, S.B., Cahoon, D.R., Lynch, J.C., and Rafferty, P., 2014, Below the disappearing marshes of an urban estuary: Historic nitrogen trends and soil structure: Ecological Applications, v. 24, no. 4, p. 633–649.

Williams, H.F.L., and Flanagan, W.M., 2009, Contribution of Hurricane Rita storm surge deposition to long-term sedimentation in Louisiana coastal woodlands and marshes: Journal of Coastal Research Special Issue 56, p. 1671–1675.

Williams, S.J., Arsenault, M.A., Buczkowski, B.J., Reid, J.A., Flocks, J.G., Kulp, M.A., Penland S., and Jenkins, C.J., 2006, Surficial sediment character of the Louisiana offshore Continental Shelf region: A GIS compilation: U.S. Geological Survey Open-File Report 2006–1195.

Xu, K., Mickey, R.C., Chen, Q., Harris, C.K., Hetland, R.D., Hu, K., and Wang, J., 2015, Shelf sediment transport during Hurricanes Katrina and Rita: Computers & Geosciences, v. 90, part B, p. 24–39.

Xu, K.H., Sanger, D., Riekerk, G., Crowe, S., Van Dolah, R., Wren, P., and Ma, Y., 2014, Seabed texture and composition changes offshore of Port Royal Sound, South Carolina before and after the dredging for beach nourishment: Estuarine, Coastal and Shelf Science, v. 149, p. 57–67. DOI: 10.1016/j.ecss.2014.07.012.

Zhao, H., and Chen, Q., 2014, Modeling attenuation of storm surge over deformable vegetation: Methodology and verification: Journal of Engineering Mechanics, DOI: 10.1061/(ASCE)EM.1943-7889.0000704.

Zhao, H., and Chen, Q., 2016, Modeling attenuation of storm surge over deformable vegetation: Parametric study: Journal of Engineering Mechanics, DOI: 10.1061/(ASCE)EM.1943-7889.0001109.

Publishing support provided by:
Lafayette Publishing Service Center

For more information concerning this publication, contact:
Director
Wetland and Aquatic Research Center (WARC)
U.S. Geological Survey
7920 NW 71st Street
Gainesville, FL 32653

Or visit the WARC website at:
https://www.usgs.gov/centers/wetland-and-aquatic-research-center-warc

ISSN 2331-1258 (online)
https://doi.org/10.3133/ofr20171016